Potential of the reversed-inject differential flow modulator for comprehensive two-dimensional gas chromatography in the quantitative profiling and fingerprinting of essential oils of different complexity

Potential of the Reversed-Inject Differential Flow Modulator for Comprehensive Two-dimensional Gas Chromatography in the Quantitative Profiling and Fingerprinting of Essential Oils of different complexity

Chiara Cordero[1*], Patrizia Rubiolo[1], Luigi Cobelli[2], Gianluca Stani[2], Armando Miliazza[3], Matthew Giardina[4], Roger Firor[4], Carlo Bicchi[1]

[1]Authors' affiliation:

[1]Dipartimento di Scienza e Tecnologia del Farmaco, Università di Torino, Turin, Italy

[2]SRA Intruments SpA, Cernusco sul Naviglio, Milan, Italy

[3]Agilent Technologies Italia SpA, Cernusco sul Naviglio, Milan, Italy

[4]Agilent Technologies, Wilmington DE, USA

* Address for correspondence:

Prof. Dr. Chiara Cordero - Dipartimento di Scienza e Tecnologia del Farmaco, Università di Torino, Via Pietro Giuria 9, I-10125 Torino, Italy – e-mail: chiara.cordero@unito.it ; phone: +39 011 6707662; fax: +39 011 2367662

Abstract

In this study, the first Capillary Flow Technology reverse-inject differential flow modulator was implemented with different column configurations (lengths, diameters and stationary phase coupling) and detector combinations (Mass Spectrometry -MS and Flame Ionization Detection - FID) to evaluate its potential in the quantitative profiling and fingerprinting of medium-to-highly complex essential oils. In particular, a parallel dual-secondary column dual-detection configuration, that has shown to improve the information potential also with thermally modulated GC×GC platforms (MS identification reliability and accurate FID quantitation), was tested. Several system performance parameters (separation measure $S_{GC\times GC}$, Modulation Ratio M_R, separation space used and peak symmetry) were evaluated by analyzing a mixture of volatiles of interest in the flavor and fragrance field. The systems demonstrating the best chromatographic performance were selected for quantitative profiling of lavender and mint essential oils and fingerprinting of vetiver essential oil. Experimental results demonstrate that careful tuning of column dimensions and system configurations yields improved: (a) selectivity ; (b) operable carrier gas linear velocities at close-to-optimal values; (c) ^{2}D separation power by extending the modulation period; and (d) handling of overloaded peaks without dramatic losses in resolution and quantitative accuracy.

Key-words:

Two-dimensional comprehensive gas chromatography-mass spectrometry and flame ionization detection; reverse-inject differential flow modulation; quantitative profiling; fingerprinting; essential oil analysis; parallel dual secondary column-dual detection

1. Introduction

Analysis of natural complex mixtures of volatiles is one of the most important fields of application of gas chromatography (GC) and related techniques [1]. GC is usually applied (*a*) to characterize sample composition, (*b*) to quantify informative analytes or (bio)-markers such as toxic compounds, regulated substances (e.g. volatile suspected allergens) or potent odorants (e.g. key-aroma compounds), and (*c*) to detect adulterations.

A common compositional characteristic of plant volatile fractions is the variable nature and abundance of constituents [from traces (ng/g) to some percent (g/100g)], which mainly consists of secondary metabolites (mono- and sesquiterpenoids, volatile phenols, etc.) and groups of chemically-correlated components such as alcohols, carbonyl derivatives, acids and esters, and volatile phenolic derivatives. Post-harvest treatments and/or technological processing further increase chemical complexity because of the thermal-induced or biologically-catalyzed reactions that impacts on native constituents. These compounds sometimes show similar chromatographic retention behavior and are characterized by MS fragmentation patterns with several common isobaric ions (fragments) that make their mono-dimensional characterization and quantitation challenging.

When the Giddings' definition of sample dimensionality [2] is applied to samples of vegetable origin (essential oils, extracts and volatiles fraction), "*the number of independent variables that must be specified to identify the components"* is generally very high and very frequently exceeds that of the analytical system. In such cases, it is necessary to adopt multidimensional analytical platforms (multiple analytical dimensions) to obtain resolved, rational and informative separation patterns.

Moreover, when GC is adopted in the context of modern *omics* investigations to study the complex biological phenomena of plant cross-talking and food sensory perception, such as in plant volatilomics [3] or food sensomics [4], the analytical information must be reliable, quantitative and extended to all detectable and chromatographically resolved entities to give the correct informative role to each single chemical.

In this context, comprehensive two-dimensional gas chromatography (GC×GC) coupled with mass spectrometry (MS) is the technique of choice for the detailed analysis (quali-quantitative profiling) of medium-to-high complexity mixtures of volatiles of plant origin. Compared to one-dimensional systems, GC×GC applies different separation selectivity in two chromatographic dimensions thus providing higher separation power, unmatched peak capacity [5,6,7] and meaningful 2D elution patterns that facilitate analyte identification and sample fingerprinting.

Thermal modulators, and in particular those implementing a cryogenic device [8], are widely used in this field because of the sample complexity (e.g. dimensionality), and in some cases, for the pre-eminent informative role of highly volatiles (C_2-C_4 compounds) [9,10] that require a very efficient band focusing to avoid break-through phenomena. These modulators can provide a peak capacity gain (G_n) that, under optimized conditions, can be 10-20% below the theoretically achievable maximum [7]. A peak capacity gain approximately of one order of magnitude higher compared to 1D-GC has been obtained and is substantially related to the very efficient re-injection of eluting bands into the secondary column. Commercial modulators, adopting liquid nitrogen as cryo-fluid, produce under optimized conditions, re-injection bands of 20 ms width at half-height [7]. Additionally, thermal modulators are connoted by a great flexibility in terms of tuning of modulation parameters. Loading capacity, modulation period (P_M), cryo-focusing temperature (obtained by varying the cold-jet volumetric flow per unit time), hot-jet pulse temperature and duration, above all, can be optimized to match for sample components relative abundance and differential selectivity between the two chromatographic dimensions. However, thermal modulation has also some drawbacks mainly related to the high costs in term of hardware and operations and seemingly complex optimization [8,11,12] that address its application mainly to research and development studies and limits its adoption for routine quality controls and high-informative throughput screenings [13].

Differential-flow modulators (FM), and in particular those based on the original device from Seeley et al. [14,15], can be considered an interesting alternative because of their simple but effective design, their low operational costs and hardware robustness. When operating in a fully-flexible configuration [16,17], the accumulation loop can be adjusted in terms of length and diameter to avoid its overloading when extended re-injection periods are applied to obtain a secondary column volumetric gas-flow compatible with MS detection.

The first commercial differential flow-modulation device for GC×GC was introduced by Firor in 2006 [R.L. Firor, Application Brief 5989-6078EN, Agilent Technologies, 2007]. The device was fabricated using diffusion bonded Capillary Flow Technology (CFT) microfluidic plates and was based on the forward fill/flush (FFF) dynamics described by Seeley et al. [15]. Several authors demonstrated its effectiveness in some application fields: bacteria fatty acids methyl esters fingerprinting [18], hydrocarbon compounds in light cycle oils (LCO) profiling [19], gasoline and kerosene analysis [20] and volatiles profiling from roasted almonds [21] although some drawbacks for samples with widely variable abundance of components were emphasized.

111 It was evident that highly concentrated peaks overloaded the accumulation loop by producing in
112 consequence a solid streak in the second dimension at given first dimension (^{1}D) times. In such a
113 situation it is almost impossible to resolve fully the major components from trace analytes eluting in the
114 same ^{1}D region.
115 More recently, a second generation of differential flow modulation was presented [22]; this new
116 configuration, adopts a reverse fill/flush (RFF) injection dynamic instead of the FFF of the first
117 generation. Advantages include: (*a*) higher efficiency of band re-injection with improved ^{2}D peak-widths
118 and symmetry, (*b*) adjustable collection channel volume, (*c*) better handling of the overloading
119 phenomenon without dramatic loss of separation power and resolution [22,23].
120 In the present study the effectiveness of the RFF differential flow modulator for GC×GC for the detailed
121 analysis (profiling) and fingerprinting of medium-to-highly complex samples of interest in the flavor and
122 fragrance field is investigated. In particular: a model mixture of volatiles and essential oils of different
123 complexity (mint, lavender and vetiver essential oils) were chosen as challenging examples. Keeping
124 constant the accumulation loop volume and the dynamics of the modulator operation (e.g. RFF), column
125 dimensions (^{1}D and ^{2}D column lengths and diameters), column configuration (stationary phase
126 chemistry combination and film-thickness) and detection (MS and Flame Ionization Detection - FID)
127 were varied. System effectiveness was tested in terms of:
128 (*a*) separation power through the separation measure ($S_{GC\times GC}$) parameter and number of separated
129 peaks above a fixed threshold;
130 (*b*) selectivity exploitation and occupation of the available separation space;
131 (*c*) quantitation reliability with FID predicted response factors (*PRF*) [24];
132 (*d*) fingerprinting effectiveness for complex samples.
133
134 **2. Experimental**
135 **2.1 Essential Oils (EO) samples, pure reference compounds and solvents**
136 Pure standards of *n*-alkanes (from *n*-C9 to *n*-C25) for Linear Retention Indices (I^T_S) calibration and for
137 Internal Standardization (ISTD) were from Sigma-Aldrich (Milan, Italy). Pure standards of volatiles of
138 interest in the flavor and fragrance field listed in **Table 1** and those adopted for external calibration and
139 FID Predicted Response Factors quantitation accuracy assessment were from Sigma-Aldrich (Milan, Italy)
140 or from authors' laboratory.
141 Solvents (cyclohexane and dichloromethane) were all HPLC-grade from Sigma-Aldrich (Milan, Italy).

142 *Mentha* x *piperita* L. EO (peppermint) was prepared in agreement to the method of the European
143 Pharmacopoeia [25] and kindly supplied by Dr. Franco Chialva (ChialvaMenta, Pancalieri, Turin Italy).
144 *Mentha spicata* L., *Lavandula angustifolia* Mill. EO (lavender) and *Lavandula angustifolia* Mill. x
145 *Lavandula latifolia* Medik (lavandin Grosso) were purchased from the market.
146 *Chrysopogon zizanioides* (L.) Roberty (formerly known as *Vetiveria zizanioides* (L.) Nash) EOs from
147 different geographical origins (i.e., *Haiti*, *Brazil*, *Bourbon* and *Java* type) were kindly provided by Prof.
148 Massimo Maffei (University of Turin, Italy).
149
150 **2.2 Calibration solutions and EO samples dilutions**
151 Standard stock solutions of reference analytes for performance evaluation (Volatiles Model Mixture -
152 VMM), identity confirmation and external calibration were prepared at a concentration of 10 mg/mL in
153 dichloromethane or cyclohexane and stored at -18°C.
154 VMM was prepared at a final concentration of 50 mg/L by diluting suitable volumes of Standard Stock
155 Solutions in cyclohexane.
156 Calibration solutions for EOs quantitative profiling and accuracy evaluation of 1,8-cineole, borneol,
157 camphor, carvone, iso-menthone, isopulegol, lavandulol, limonene, linalyl acetate, lavandulyl acetate,
158 limonene, linalool, menthol, menthone, menthyl acetate, neo-isomenthol neo-menthol, pulegone and
159 terpinen-4-ol were prepared by diluting suitable volumes of Standard Stock Solutions at final
160 concentrations of 250, 200, 150, 100, 75, 50, 25, 20 and 10 mg/L in cyclohexane.
161 Peppermint, spearmint, lavender and vetiver EO samples were prepared at different final
162 concentrations (10, 5, 2, and 1 mg/mL and 500 µg/mL) in dichloromethane or cyclohexane to comply
163 with the detector linearity range and afford FID predicted response factors (PRF) quantitation
164 requirements.
165 Standard stock solutions of ISTDs (*n*-tetradecane, *n*-pentadecane and *n*-hexadecane) at a concentration
166 of 50 mg/L were added to the investigated samples to normalize responses and afford FID PRF
167 quantitation.
168
169 **2.3 GC×GC instrument set-up**
170 GC×GC analyses were run with a system consisting of an Agilent 7890B GC unit provided with a 4513A
171 auto injector sampler (Agilent, Little Falls, DE, USA) coupled to an Agilent 5977A fast quadrupole MS
172 detector (Agilent, Little Falls, DE, USA) operating in EI mode at 70 eV and a fast FID detector. The GC
173 transfer line was set at 250°C or 280°C depending on the ^{2}D stationary phase and maximum operative

temperature. The MS was tuned using the automated Extraction Source Tune (*Etune*) algorithm. The scan range was set to m/z 40-250 with a scanning rate of 20,000 amu/s to obtain a spectra generation frequency of 35 Hz. The Flame Ionization Detector (FID) conditions were: base temperature 280°C, H_2 flow 40 mL/min, air flow 240 mL/min, make-up (N_2) 450 mL/min, and sampling frequency 150 Hz.

Injections of the EOs and of reference mixture, as well as those for I^T_S determination, were carried out with a 4513A auto injector under the following conditions: split/splitless inlet, split mode, split ratio 1/40, injection volume 1µL, and inlet temperature 280°C.

Analytes identification and/or identity confirmation was by matching MS spectra to those collected in commercial databases and verifying coherence of experimental I^T_S with tabulated ones.

2.4 Differential flow modulator operative principle and parameters

The system was equipped with a reverse-inject differential flow modulator (**Supplementary Figure S1**) consisting of one CFT plate connected to a three-way solenoid valve that receives a controlled supply of carrier gas (helium) from an auxiliary electronic pressure control module (EPC). The CFT plate, graphically depicted in **Figure 1A** (loading stage) and **Fig. 1B** (injection stage), has three-ports for connection of the first and second dimension columns and bleed capillary. The collection channel is etched into the plate itself.

Analytes separated into the ^{1}D column enter at the center port of the modulator plate (Column 1 in) and fill the fixed size collection channel which is connected to the bleed capillary port (bottom port). This occurs for typically 2-5 seconds at a first dimension column flow of 0.3 to 0.5 mL/min. Bleed (or restrictor) capillary enables the carrier gas to pass through the accumulation capillary during the fill cycle and allows a reversal of flow direction during the flush cycle. Length and diameter of the bleed capillary are chosen according to pressure/flow conditions of columns to provide flow equivalent to the output of the first dimension.

After the loading of the collection channel, the three-way solenoid micro valve switches EPC module flow to the bottom post, the channel is flushed for typically 0.10-0.20 seconds in the reverse direction of the fill flow into the ^{2}D column at a suitable volumetric flow. The band enters into the ^{2}D column and undergoes to separation in few seconds. The modulation cycle is then repeated.

2.5 Column set, connections and auxiliary control module

Column set adopted are summarized in **Table 2** together with initial head-pressure settings (S/SL injector and EPC) and corresponding carrier gas (helium) volumetric flows and linear velocities. Oven temperature programming is also reported.

Connection between the CFT plate and the two secondary columns was by a three-way unpurged splitter (G3181B, Agilent, Little Falls, DE, USA) while deactivated silica capillaries were connected by deactivated ultimate unions (G3182-61580 Agilent, Little Falls, DE, USA). All columns and capillaries were from Agilent - J&W (Little Falls, DE, USA).

2.6 Data acquisition and 2D data automatic processing

Data were acquired by – Enhanced MassHunter (Agilent Technologies, Little Falls, DE, USA) and processed using GC Image® GC×GC Edition Software, Release 2.5 (GC Image, LLC Lincoln NE, USA).

3. Results and Discussion

After a short discussion on the rationale behind the system tuning, this section reports the experimental results on several parameters of system performance (re-injection pulse width $^2\sigma_i$, separation measure $S_{GC\times GC}$, modulation ratio M_R and separation space used) for volatiles of interest in the flavor and fragrance field (VMM) analyzed with different column configurations under optimized conditions. The second part is dedicated to real-world sample analysis. EOs differing in complexity and composition were chosen as examples of routine GC×GC application to evaluate the system potential to obtain both a full quantitative profiling by FID-RRF and a reliable fingerprinting for classification purposes.

3.1 Systems set-up: rationale behind column settings and analysis conditions

In this section, the logical approach to the set-up and evaluation of five different GC×GC configurations is discussed. As a first step the manufacturer's suggested configuration was implemented (Set-up I); it consists of a conventional 30 m × 0.25 mm d_c ^{1}D column coupled with a homologue diameter short column (e.g., 2.5 m × 0.25 mm d_c) coated with different stationary phases (^{1}D: SE52, ^{2}D: OV1701). A splitter was connected at the end of the secondary column to afford a dual detection by FID and MS. Two deactivated capillaries were used to divert the effluent to the detectors (FID and MS) with a 75:25 ratio. This condition was necessary because of the relatively high ^{2}D volumetric flow necessary to flush the filling capillary; thus to comply with MS pumping capacity it had to be reduced to a maximum of about 6-7 mL/min.

Although effective when looking at the separation pattern of the VMM analytes (**Figure 2A**), this configuration has some drawbacks mainly related to the very low ^{1}D average carrier velocity (about 5 cm/s) that results in longer analysis time (sclareol elutes after 75 min) and limited separation performances; this aspect may be relevant for the separation of critical pairs.

The next configuration (e.g., Set-up II) included a narrow-bore ^{1}D column (10 m × 0.10 mm d_c × 0.10 µm d_f) with the same polarity and phase ratio (β) as that of Set-up I, but coupled with two parallel ^{2}D columns with the same internal diameter. This new set up enabled the ^{1}D column to work at a closer-to-optimal carrier gas flow conditions, and at the same time, the two ^{2}D columns to operate at flows compatible with MS detection without affecting system sensitivity. The resulting 2D pattern related to the VMM separation is shown in **Figure 2B**. The peak distribution over the 2D space is coherent with that obtained by Set-up I, but some critical pairs are not adequately resolved in both dimensions.

The successive configuration (e.g. Set-up III) aimed at improving system performances in terms of ^{1}D loading capacity, therefore the overall sensitivity, and ^{2}D effectiveness. These objectives were achieved by increasing the ^{1}D film thickness, from 0.10 µm to 0.40 µm that resulted in a gain of 4 times the loading capacity, and ^{2}D column(s) length (from 1.0 to 1.5 m). Longer ^{2}D columns enabled to reduce of the carrier gas volumetric flow from the ^{2}D and to increase the modulation period (from 2.5 s to 4 s) to better exploit the ^{2}D selectivity. **Figure 2C** illustrates the 2D pattern of VMM analytes obtained with Set-up III after having tuned analysis conditions (temperature rate and modulation period). Results were satisfactory and suggested to evaluate the effect of a more polar ^{2}D stationary phase: the possibility to extend the modulation period (P_M) to 4 seconds without detrimental effects on modulation (overloading of the collection channel and consequent streaking) should afford operation at faster temperature rates with a reduction of the analysis time.

Set-up IV consisted of a ^{1}D apolar column (OV1 10 m × 0.10 mm d_c × 0.40 µm d_f) coupled with two parallel ^{2}D polar columns coated with PEG20M (1.5 m × 0.10 mm d_c × 0.10 µm d_f). The orthogonality of the system increased with a clear influence on the overall performances (**Figure 2D**); this set up was thus adopted for the fingerprinting of Vetiver EOs, a very complex mixture plant secondary metabolites mainly consisting of sesquiterpenoids (see section 3.4).

A column configuration widely employed in the flavor and fragrance field was at last tested, i.e. a ^{1}D polar column (i.e. coated with PEG) coupled with a ^{2}D intermediate polarity column (i.e., OV1701). Set-up V was used for the VMM separation, mint and lavender EOs profiling (see section 3.3). **Figure 2E** reports the VMM analytes separation pattern where it is clear that the spreading of the peaks over the

chromatographic space is excellent as well as peak shapes and peak-widths, although the primary separation is here driven by a combination of volatility/polarity resulting in a different 2D pattern.

3.2 Systems performance evaluation

Several performance parameters were evaluated to compare the effectiveness of each investigated set-up for applications in the field of plant volatile secondary metabolites and odor active compounds, after having explored the best analysis conditions for each column combination (carrier gas flow-rates, oven temperature programming, P_M and injection time) with the primary objective of the full separation of target analytes in the shortest analysis time.

The first estimated parameter, at the basis of system performance, was the re-injection pulse width (σ^2_i). This parameter strongly affects the second dimension separation effectiveness since too wide injection pulses directly affect the actual σ^2_t [26] with a broadening effect that is additive to the chromatographic one (σ^2_c).

Re-injection pulses were calculated, according to the procedure proposed by Klee et al. [7], by integrating un-retained solvent peaks (streaking) in the middle of the 2D chromatogram in the FID channel (operating at 100 Hz sampling frequency) and reporting them as peak standard deviation ($^2\sigma_i$). It can be assumed that solvent (cyclohexane) pulses at high temperatures are not retained by the ^{2}D column. Values are reported in **Table 3** and refer of very effective re-injection bands thanks to the geometry of the CFT plate and of the re-injection dynamics (e.g., RFF). These values are in perfect agreement with those reported by Duhamel et al. [23] that studied the effectiveness of FFF and RFF dynamics for the analysis of vacuum distilled mineral oils.

The net separation measure ($S_{GC\times GC}$) was assumed as quantitative descriptor of the system separation ability, under the experimental conditions applied. The separation measure, S, introduced by Blumberg et al. [27], was calculated using the following equation (**Equation 1**):

$$S = \Delta t \sigma_{av} \qquad \textbf{Eq. 1}$$

where Δt is the arbitrary time interval limited by two peaks a and b, $\Delta t = t_b - t_a$, and σ_{av} is the average σ of a and b (**Equation 2**):

$$\sigma_{av} = \frac{(\sigma_a + \sigma_b)}{2} \qquad \textbf{Eq. 2}$$

The net separation measure ($S_{GC\times GC}$) extended the *S* concept to GC×GC separations [28], and is the product of the separation measure of each chromatographic dimension (Equation 3):

$$S_{GC\times GC} = S_1 \times S_2 \qquad \textbf{Eq. 3}$$

This parameter indicates the separation power of each GC×GC column combination, considering the average σ values in both chromatographic dimensions estimated for the separation of the VMM sample. **Table 3** reports $S_{GC\times GC}$ together with absolute retention times (^{1}D Rt and ^{2}D Rt in seconds) of the first and last eluting analytes for each column set, the ^{1}D and ^{2}D σ values in seconds (based on peak variances calculated by GC-Image software), *S* for each chromatographic dimension, $S_{GC\times GC}$ and $S_{GC\times GC}$ normalized to the analysis time (t_A). This last parameter was introduced to make the system efficiency evaluation independent of the analysis time.

Experimental data indicate that in terms of separation power, ^{1}D columns behave almost similarly with some exceptions; S_1 ranges between a minimum of 474 for Set-up III (^{1}D SE52 10 m × 0.10 mm d_c - ^{2}Ds OV1701 1 m × 0.10 mm d_c) and a maximum of 772 of Set-up V (^{1}D PEG 10 m × 0.10 mm d_c - ^{2}Ds OV1701 1.5 m × 0.10 mm d_c) where the volatility/polarity driven separation of the ^{1}D is very effective for the selected analytes. Larger differences are evident for net ^{2}D performance, Set-up I adopting a 5 m × 0.25 mm d_c secondary column, although operating at very high flow-rate, produces wider peaks and shows a poor orthogonality thus leading to shorter P_M (2.5 seconds instead of 4 to 5 s used for more "orthogonal" combinations), thus directly affecting the separation measure of this dimension. The two best performing set-up in terms of net separation measure ($S_{GC\times GC}$) are not surprisingly those where the two separation mechanisms were more orthogonal because driven by different secondary interactions (Set-up V) or where the selectivity of the secondary column was better exploited (Set-up III).

These results are perfectly comparable in terms of ^{2}D performances to those obtained with a thermal modulator and a stationary phase set similar to that of Set-up III [29] (S_2 of 43 instead of 38 in the present study).

Modulation Ratio (M_R) was the third investigated performance parameter. Mathematical models on the modulation process of symmetrical Gaussian peaks [30] show that, an M_R of at least 3 is required to obtain a good degree of confidence for the area determination for trace analytes (S/N ratio of 3) while an M_R of 1.5 is sufficient to quantify abundant analytes (S/N ratio of 10) and/or for screening analyses. The number of detectable modulated pulses, considering both in-phase and out-of-phase modulations,

is always between 2 and 3 for symmetrical peaks with a corresponding M_R value of 1, while it increases to 4 when asymmetrical peaks are considered [30].

M_R was calculated using the equation proposed by Khummueng et al. [30] (**Equation 4**):

$$M_R = \frac{4\sigma}{P_M} = \frac{W_b}{P_M} = \frac{4W_h}{P_M 2.35} \qquad \textbf{Eq.4}$$

where W_h and W_b are the half-height and the baseline peak width of the 1-D Gaussian peak (assumed to be symmetrical), and P_M is the modulation period.

Table 3 reports M_R calculated for the first- and last-eluted components of the VMM sample and for all column set. M_R always complies with the minimum value (e.g. 3) with the only exception of α-pinene analyzed with Set-up V; this monoterpene is eluted in a very narrow band from the ^{1}D that exerts a minimal retention on this hydrocarbon.

The survey on systems effectiveness was completed by evaluating the component distribution over the 2D plane through the amount of separation space used [29,31]. This parameter measures the ratio between the 2D area occupied by solute separation (between the first and the last eluted analytes in both dimensions) and the 2D available area that is reduced by the unused separation space beneath the second dimension (i. e. the hold-up time). This parameter is a direct expression of the degree of correlation between the two dimensions that depends not only on the nature of the stationary phase combination but also on the selectivity tuning operated by temperature programming.

The histogram in **Figure 3A** graphically represents the amount of separation space used calculated according to Ryan *et al*. [31] and the corresponding pixel-based area ratios calculated by dividing the boundary area (pixels counts) defined around the elution pattern of VMM analytes (darker boundary in **Figure 3B**) and the available retention time area (lighter boundary in **Figure 3B**). These results integrate the evaluation of the system effectiveness giving a more realistic view on their overall performances: Set-up II connoted by a lower ^{2}D peak-capacity, also due to the P_M adopted (i.e., 2.5 s), compensates this limitation with a good selectivity exploitation that results in a good peak-spreading over the chromatographic space.

System performances, related to single VMM analytes, are reported in **Table 4** and include also ^{1}D and ^{2}D peaks symmetry and peak variances.

3.3 Real-world samples: quantitative profiling of medium complexity essential oils

Although complex and time-consuming, essential oils quantitative profiling has some important advantages even when not mandatorily required for regulated substances (e.g., suspected allergens or toxic compounds), deriving from: (*a*) the possibility to unequivocally define the product quality related to a reference standard; (*b*) the possibility of data comparison over an extended time frame, varied instrumentation and laboratories; (*c*) the definition of the biological role of (potential) biomarkers.

GC×GC is a technique of great interest for complex samples because of the ability to provide "fully" resolved, unique and particular peak patterns (chromatographic fingerprint). Moreover, the availability of a GC×GC-FID output for a full quantitative assessment and of GC×GC-MS for confirmatory purposes increase its attractiveness.

The challenges to quantifying the large number of peaks generated by GC×GC can be overcome by adopting FID predicted response factor(s) (FID-PRFs) based on combustion enthalpies and molecular structures [24]. This approach enables analyte quantitation without external standards.

The approach was introduced by de Saint Laumer *et al.* [24] and applied to vetiver EOs qualification by GC×GC-FID by FIlippi et al. [32] and to mint and lavender EOs quantitative profiling by GC×2GC-FID/MS by Sgorbini et al. [33]. The latter instrumental configuration, that inspired the current set-up implemented with the differential flow-modulation GC×GC, provides data for simultaneous analyte identification (EI-MS full spectrum) and quantitation (MS single ions and FID responses) with possibility of an internal cross-validation of the results [34]. The effective alignment of the separation patterns obtained with the two detectors at the data elaboration level strengthens the complementarity and reliability of the results.

In this study, the reliability of the GC×2GC-FID/MS with differential flow modulation for the quantitative assessment of mint and lavender EOs was evaluated. Set-up V combining a polar column in the ^{1}D and a medium polarity phase in the ^{2}D was adopted. Analyte identification was obtained by matching EI-MS spectra to those of commercial databases (MS Identity Match Factor above 850 - NIST Algorithm) and verifying coherence of experimental I^{T}_{S} with the tabulated ones.

Table 5 reports the list of marker components identified in mint EO samples (*Mentha* x *piperita* L. and *Mentha spicata* L.) while **Table 6** those of lavender EOs (*Lavandula angustifolia* Mill. and *Lavandula angustifolia* Mill. x *Lavandula latifolia* Medik) together with average retention times in the two chromatographic dimensions (^{1}D Rt and ^{2}D Rt) and their coefficient of variation (CV% over six replicates), FID Normalized 2D Volumes (over ISTD *n*-pentadecane at 25 mg/L), Normalized 2D Volumes percentage and quantitative results (g/100g) obtained by FID PRF or by External Calibration including also the

quantification error or *bias*, are reported as Recovery % (i.e. the ratio between the amount estimated by FID PRF vs. the result of the external calibration).

Predicted RRFs were calculated according to the reference formulae [24] and normalized to *n*-pentadecane, here adopted as an ISTD for normalization.

The quality control of *Mentha* spp. EOs focuses on a series of authenticity markers which are reported in literature as having a given quantitative profile. Area Percentage (Area %) of limonene, 1,8-cineole, menthone, menthofuran, isomenthone, menthyl acetate, isopulegol, menthol, pulegone, and carvone are listed as quality markers in the European Pharmacopoeia [25], in the United States Pharmacopeia (USP), and in ISO References for peppermint EOs (*Mentha* x *piperita* L., Lamiaceae). In addition, isopulegol plays a crucial role in the authentication and/or adulteration assessment of peppermint with *Mentha arvensis* L. (cornmint) [35]. (*R*)-(-)-carvone is a quality marker of *Mentha spicata* (native spearmint) and *Mentha* x *gentilis* (scotch spearmint) because of its distinctive odor note [35].

The 2D separation patterns of peppermint and spearmint are shown in **Figures 4A** and **B** where marker peaks are baseline resolved from other components. The high efficiency of Set-up V in addition to the use of two parallel capillaries to double loadability enable both reliable separation and quantitation in the elution regions of both menthols for peppermint (**Figure 4A),** and carvone and its derivatives for spearmint (**Figure 4B).** These analytes have similar retention behavior on the ^{1}D stationary phase (*e.g.*, PEG), but their correct separation might be affected by other phenomena (e.g. column overloading) with detrimental effects on identification/quantitation of minor peaks eluting in the proximity of highly abundant components (*e.g.* neoisomenthol and pulegone *vs.* menthol). Quantitative results on target peaks and quality control markers of mint spp. EOs are reported in **Table 5** and show a perfect agreement between quantitative data obtained by external calibration and FID-PRF; the relative error (accounted as bias) never exceeded +/-22% .

In the perspective of quality assessment, experimental results confirm that the *Mentha* x *piperita* EO profile is in agreement with the European Pharmacopeia specifications for both: (a) markers percentage areas distribution and (b) 1,8-cineole/limonene ratio (reference ratio ≥ 2). Isopulegol content (0.07 %) is in agreement with that of authentic peppermint reference samples [25].

Similar analyses can be done for lavender EOs; here the number of detected components above a fixed threshold (i.e. SNR>25 at FID channel) was higher, 280 2D-peaks instead of 230 detected on peppermint and spearmint EOs.

The quality control (QC) of lavender EOs focuses on a series of authenticity markers requiring a quantitative profiling approach. Area Percentage (Area %) values and/or intervals are reported for linalool, linalyl acetate, lavandulyl acetate, 4-terpineol, lavandulol, 1,8-cineole, camphor, and borneol in the European Pharmacopoeia [25] and in some ISO References for *Lavandula angustifolia* Mill. and for *Lavandula angustifolia* Mill. x *Lavandula latifolia* Medik. (lavandin "grosso") [36].

Quantitative results on target peaks and QC markers of lavender spp. EOs are reported in **Table 6** while the separation patterns are shown in **Figures 4C** and **4D.** Quantitative data indicate a good agreement between external calibration and FID-PRF results. 2D Volume % confirm that lavandin EO chemical pattern is coherent with the ISO Reference [37], as well as for the *Lavandula angustifolia* sample that shows a profile compatible with the European Pharmacopeia reference.

The confirmatory role of the MS detector is fundamental, and although the operating carrier gas flows are high with a detrimental effect on detection sensitivity, the characterizing components of the EOs can be confirmed by their characteristic fragmentation pattern combined with ^{1}D linear retention indices (I^{T}_{S}).

Figure 5 shows the alignment of the two detector channels (MS black trace - FID blue trace) at the elution region of camphor; the SNRs values are perfectly comparable (258 vs. 304) although, as expected, the absolute noise at the MS channel is higher than under normal conditions with outlet flows of 1-2 mL/min.

3.4 Untargeted fingerprinting of complex mixtures

After having confirmed the system reliability for quantitative profiling of medium-complexity EOs (about 250-300 2D peaks SNR>25) the system potential for untargeted fingerprinting on more complex mixtures was investigated. The samples adopted for this part of the study are vetiver EOs (*Chrysopogon zizanioides* (L.) Roberty) of different geographical origins (Haiti, Indonesia, Brazil and La Réunion) that corresponds to different "types": *Haiti*, *Java*, *Brazil* and the *Bourbon*, the latter is considered as a reference for high quality products [38].

Vetiver EO composition is characterized by a complex sesquiterpenoid fraction that includes hydrocarbons, alcohols, aldehydes, ketones, and acids [32,38]. These constituents can be classified in function of their sesquiterpene skeletons, i. e. eremophilanes, spiroaxanes, vetispiranes, acoranes, schamigranes, zizaanes, eudesmanes, amorphanes, murolanes, cadinanes, bisabolanes, elemanes, patchoulanes, cedranes, cyclocopacamphanes, khusianes, nigritanes, cyclogermacranes and oppositanes [38]. When analyzed in 1D-GC with apolar stationary phases, they all elute in the 1400-2050 I^{T}_{S} interval,

making very complex (if not impossible) to obtain a suitable chromatographic resolution for reliable identification and quantitation without a sample pre-fractionation [38].

The detailed profiling of vetiver EOs has been investigated with GC×GC by Marriot et al.[39] and more recently, by Filippi et al. [32], who evaluated the feasibility of a full quantitative assessment of vetiver EO samples by GC×GC-FID and FID-PRFs. Their quantitative results were validated over external calibration and experimental response factors for those components available on the market and revealed a partial incongruence to those obtained by normalized methods (ISO 4716:2013) based on 1D-GC separations [40].

In this context, the possibility to obtain highly-detailed separation patterns from vetiver EOs to be used as chemical signatures for fingerprinting and classification purposes is therefore of high interest.

Set-up IV was chosen for the vetiver EO chemical fingerprinting; its advantages are related to the volatility driven separation of the ^{1}D that enables to separate hydrocarbons from oxygenated compounds (see **Figure 6A**), while a volatility/polarity principle drives the ^{2}D separation that selectively retains carbonyls (aldehydes and ketons) from alcohols (primary, secondary and tertiary) and acids.

The selectivity of the ^{2}D was obtained by operating at different temperature rates (from 3.5 °C/min to 1.5°C/min) and the effects on the 2D peak spreading on the chromatographic plane are shown in Supplementary **Figures 2A-C** (**S2A**-rate 3.5°C/min; **S2B**-rate 2.5°C/min; **S2C**-rate 1.5°C/min). In any case, the tuning of the rate has also to consider that with quicker rates complex oxygenated fractions are not appropriately separated while with slower rates carboxylic acids wrap-around. To note, the P_M cannot further be increased to compensate the higher retention without affecting the modulation efficiency.

The EOs of *Brazil*, *Java*, *Haiti* and *Bourbon* types were analyzed and the resulting patterns compared by chromatographic fingerprinting based on image features (image comparison) and peak-region features approaches (template matching) [41]. The number of detected peaks (FID detection) above an arbitrarily fixed 2D Volume threshold of 30,000 and a SNR>25 are 583 for *Brazil*, 540 for *Java*, 553 for *Haiti* and 733 for *Bourbon*. The result of the direct comparison of the *Bourbon*-type sample *versus* the *Haiti*-type is illustrated in **Figure 6B** (*Bourbon* vs. *Haiti*). The comparative visualization, obtained after a pre-processing based on 2D chromatograms alignment and peak-region response normalization, reveals differences in the chemical pattern. In the visual comparison of **Figure 6B**, using the Hue-Intensity-Saturation (HIS) color space to color each pixel in the retention-times plane, the *colorized fuzzy difference* visualization reveals chromatographic regions where detector response variations (positive - red and negative - green) are relevant and diagnostic of quali-quantitative differences in the chemical composition. However, when a large number of samples and related 2D patterns have to be compared,

peak-region features approaches are more effective. The algorithm implemented in commercial software (Image-Investigator®, GC-Image) was successful for complex patterns investigations including breast cancer metabolomics [42], bio-oils characterization [43] and mice urine metabolite profiling [34].

The peak-region features approach consists of a sequence of operations (a detailed description is reported in literature [34,41,42,43]), run automatically by the software that includes:

step 1) detection and registration of 2D peak patterns from individual chromatograms of the set;

step 2) localization of a few peaks, named *registration peaks,* reliably matched across all samples;

step 3) alignment of sample chromatograms in the retention time domain to create a *composite chromatogram*;

step 4) definition of a pattern of *region features* from peaks detected in the composite chromatogram;

step 5) when a target chromatogram (unknown sample) is processed *registration peaks* are matched, the feature regions are aligned relative to those peaks, and the characteristics of those features (retention times, detector response and MS fragmentation pattern above all) are computed to create a feature vector for the target chromatogram;

step 6) the feature vector is then used for cross-sample analysis (e.g. classification, discriminant analysis, clustering, etc.).

The peak-region features approach cross-aligned 315 reliable 2D-peaks; **Supplementary Table S1** reports the untargeted peak-regions list and corresponding information (^{1}D and ^{2}D retention times, Normalized 2D volumes and CV% within the set of samples). Peak features connoted by the largest variation (CV% on Normalized 2D Volumes > 50%) are indicated by yellow blobs in **Figure 6C**.

Coherently with the characteristic composition of the different EOs types, differences in relative abundance were found for:

1) peak-region #30 (^{1}D Rt 32.27 min- ^{2}D Rt 0.96 s - ^{1}D I^T_S 1550 Lit 1552) corresponding to β-vetivenene, a sesquiterpenoid hydrocarbon belonging to the eremophilane family and reported to be more abundant in *Java* and *Brazil* type EOs;

2) peak-region #213 (^{1}D Rt 44.19 min- ^{2}D Rt 4.68 s - ^{1}D I^T_S 1727 Lit 1730) corresponding to khusimol a primary alcohol belonging to the zizaane family and generally more abundant in *Haiti* and *Brazil* type EOs;

3) peak-region #98 (^{1}D Rt 47.04 min- ^{2}D Rt 4.17 s - ^{1}D I^T_S 1775 Lit 1778) corresponding to (*E*)-isovalencenol, a primary alcohol belonging to the eremophilane family abundant in the *Haiti* type EOs;

4) peak-region #189 (^{1}D Rt 48.40 min- ^{2}D Rt 3.58 s - ^{1}D I^T_S 1791 Lit 1796) corresponding to β-vetivone, a ketone belonging to the vetispirane family;

5) peak-region #188 (^{1}D Rt 50.06 min- ^{2}D Rt 3.74 s - ^{1}D I^T_S 1816 Lit 1820) corresponding to α-vetivone, a ketone belonging to the vetispirane family and generally more abundant in *Haiti* type EOs.

4. Conclusions

The performance of a reverse-inject differential flow modulator based on Capillary Flow Technology for GC×GC has been evaluated and critically discussed in view of its adoption for quantitative profiling and fingerprinting of medium-to-highly complexity essential oils. In particular, the adoption of an integrated platform that includes a dual-secondary-column, dual-detection system with different column dimensions and stationary phases were very effective in terms of key-performance parameters and information potentials. Net separation measure ($S_{GC\times GC}$), modulation ratio (M_R), separation space used, peak symmetry, chromatographic repeatability in terms of 2D peak pattern/retention (CV% on ^{1}D and ^{2}D Rts - see Tables 5 and 6) and 2D peaks normalized volumes (CV% - see Tables 5 and 6) were highly satisfactory, if compared to the forward fill/flush differential flow modulator dynamics and/or to those with a full-flexible design [16,17].

The system potential for quantitative profiling of medium-complexity EOs (mint and lavender) were confirmed by the accuracy of the results; in addition, the dual parallel detection plays a fundamental role by combining identity confirmation and quantitation by MS signal with the possibility to extend quantitation to all identified components by using FID *PRFs*.

Complex mixtures with more than 500 detectable 2D peaks, within a limited retention index window (vetiver EOs), took advantage of the system peak capacity and selectivity giving reliable and informative 2D fingerprints to be exploited for sample classification and quality control.

Experimental results presented in this study, together with the acceptable operational costs, the relative ease of use and simple maintenance of CFT reverse-inject differential flow modulation GC×GC, are promising and can promote the use of this technique for routine analysis in the flavour and fragrance field.

Acknowledgements

This study was supported by Ricerca Finanziata da Università - Fondo per la Ricerca Locale (Ex 60%) Anno 2014.

Figure Captions:

Figure 1: schematic diagram of the reverse-inject differential flow modulator in loading state (A) and injection state (B).

Figures 2A-E: separation patterns of the Volatiles Model Mixture (VMM) analytes obtained with different colum set-up. **2A** Set-up I (^{1}D SE52 -30 m, 0.25 mm d_c, 0.25 µm d_f - ^{2}D OV1701 -5 m, 0.25 mm d_c, 0.25 µm d_f); **2B** Set-up II (^{1}D SE52 - 10 m, 0.10 mm d_c, 0.10 µm d_f - two parallel ^{2}D OV1701 2×(1.0 m, 0.10 mm d_c, 0.10 µm d_f)); **2C** Set-up III (^{1}D OV1 -10 m, 0.10 mm d_c, 0.40 µm d_f - two parallel ^{2}D OV1701 2×(1.5 m, 0.10 mm d_c, 0.10 µm d_f)); **2D** Set-up IV (^{1}D: OV1 - 10 m, 0.10 mm d_c, 0.40 µm d_f - two parallel ^{2}D PEG 2×(1.5 m, 0.10 mm d_c, 0.10 µm d_f)); **2E** Set-up V (^{1}D PEG - 10 m, 0.10 mm d_c, 0.10 µm d_f - two parallel ^{2}D OV1701 2×(1.5 m, 0.10 mm d_c, 0.10 µm d_f)). For analysis conditions see details in Table 2.

Figures 3A-B: **3A** histogram reporting the separation space used and the area ratio (pixel counts) for all column set-ups. A graphical representation of the pixel-based area ratio estimation is shown in **Fig. 3B** and is obtained by dividing the boundary area (pixels counts) defined around the elution pattern of VMM analytes (darker boundary) and the available retention time area (lighter boundary).

Figures 4A-D: 2D plots corresponding to peppermint essential oil (**4A**), spearmint EO (**4B**), lavender EO (**4C**) and lavandin EO (**4D**). The Internal Standard Peak (ISTD - nC15) is graphically connected with the 2D peaks of marker compounds (see Tables 5 and 6) quantified by predicted FID response factors (PRF). Enlarged areas show the chromatographic regions where elute EOs major compounds.

Figure 5: overlapped signals from parallel detection channels (i.e., MS and FID) for camphor (lavender EO) and Signal to Noise results.

Figures 6A-C: 2D plot of vetiver EO from Haiti (**6A**) and corresponding elution regions of sesquiterpenoid derivatives (according with [32]). **Fig. 6B** comparative visualization of a Bourbon type vs. Haiti type EOs the pixel hue is set to green when the difference is positive and red when it is negative. When the difference is small, the color saturation is low, producing a grey level from black to white depending on intensity. Peaks with large differences therefore appear red or green and peaks with small differences appear white or grey. **Fig. 6C** evidences the 2D peak regions connoted by the larges variation between vetiver samples considered.

583 **Table Captions:**

584 **Table 1:** list of analytes included in the test mixture (Volatiles Model Mixture - VMM) adopted for
585 system performance evaluation. Analytes are ordered according to their chemical class and
586 functionality. ^{1}D and ^{2}D retention times (Rt) are reported for all column combinations.

587

588 **Table 2**: column set adopted, initial head-pressure settings (S/SL injector and EPC) and corresponding
589 carrier gas (helium) volumetric flows and linear velocities estimated on the basis of reference equations.
590 Oven temperature programming is also reported.

591

592 **Table 3:** performance parameters calculated on the VMM analytes for each column set-up. Data include:
593 re-injection pulse width referred as peak standard deviation (ms), first and last eluted peaks σ in both
594 chromatographic dimensions, Modulation Ratio (M_R), separation measure for each dimension (S_1 and S_2)
595 and net separation measure ($S_{GC\times GC}$), separation space used and % of usage of the separation space
596 available estimated according to Ryan *et al.* [31] or based on pixels counts (see text for details).

597

598 **Table 4:** general performance parameters for VMM analytes: 1D and 2D peak symmetry and peak
599 variances.

600

601 **Table 5**: list of marker components identified in mint EO samples (*Mentha* x *piperita* L. and *Mentha*
602 *spicata* L.) together with average retention times in the two chromatographic dimensions (^{1}D Rt and ^{2}D
603 Rt), coefficient of variation (CV% over six replicates), FID Normalized 2D Volumes (over ISTD *n*-
604 pentadecane at 25 mg/L) and CV% over six replicates, Normalized 2D Volumes percentage and
605 quantitative results (g/100g) obtained by FID PRF or by External Calibration, quantification error (i.e.,
606 bias) expressed as Recovery % and calculated as ratio between the amount estimated by FID PRF vs.
607 external calibration .

608

609 **Table 6**: list of marker components identified in lavender EO samples (*Lavandula angustifolia* Mill. and
610 *Lavandula angustifolia* Mill. x *Lavandula latifolia* Medik - Lavandin) together with average retention
611 times in the two chromatographic dimensions (^{1}D Rt and ^{2}D Rt), coefficient of variation (CV% over six
612 replicates), FID Normalized 2D Volumes (over ISTD *n*-pentadecane at 25 mg/L) and CV% over six
613 replicates, Normalized 2D Volumes percentage and quantitative results (g/100g) obtained by FID PRF or
614 by External Calibration,

615 quantification error (i.e., bias) expressed as Recovery % and calculated as ratio between the amount
616 estimated by FID PRF vs. external calibration .

Table 1

				Set-up I		*Set-up II*		*Set-up III*		*Set-up IV*		*Set-up V*	
	Chemical Class II	**Analyte**	**CAS-Registry**	**1D Rt (min)**	**2D Rt (s)**	**1D Rt (min)**	**2D Rt (s)**	**1D Rt (min)**	**2D Rt (s)**	**1D Rt (min)**	**2D Rt (s)**	**1D Rt (min)**	**2D Rt (s)**
alcohols	aromatics	Benzyl alcohol	100-51-6	22.09	1.33	8.13	1.93	14.00	2.13	11.50	3.63	22.53	1.17
	terpenoid	Linalool	78-70-6	24.88	0.70	9.63	1.45	17.13	1.84	13.50	1.67	15.47	1.62
	terpenoid	Menthol	1490-04-6 / 89-78-1 / 2216-51-5	28.71	0.91	11.59	1.55	20.67	1.94	15.92	1.73	17.80	1.80
	terpenoid	α-Terpineol	98-55-5	29.63	0.91	12.13	1.66	21.40	1.97	16.17	2.39	18.80	1.63
	terpenoid	Citronellol	106-22-9 / 1117-61-5 / 7540-51-4	30.80	0.91	13.17	1.52	21.67	1.97	16.25	1.86	20.47	1.53
	aromatics	Cinnamyc alcohol	104-54-1	34.92	1.57	14.67	2.35	24.53	2.17	19.08	1.62	30.33	1.19
	aromatics	Eugenol	97-53-0	37.34	1.22	16.55	2.04	28.40	2.26	20.58	3.69	28.33	1.31
	aromatics	Isoeugenol (*E*)	97-54-1	41.50	1.33	18.88	2.07	32.33	2.36	23.00	4.18	31.53	1.29
	terpenoid	α-(*Z*)-santalol	115-71-9 and 77-42-9 resp	51.34	0.98	24.21	1.73	42.13	2.02	29.25	1.93	31.47	1.63
	terpenoid	(*E,Z*)-Farnesol	4602-84-0	51.67	0.80	24.71	1.66	42.60	1.95	30.00	1.43	31.20	1.67
	terpenoid	β-(*Z*)-santalol	115-71-9 and 77-42-9 resp	52.67	1.01	25.17	1.80	43.53	2.06	30.33	2.01	31.93	1.64
	terpenoid	(*E,E*)-Farnesol	4602-84-0	52.71	0.84	25.25	1.62	43.53	1.95	30.17	1.76	31.73	1.62
	terpenoid	Sclareol	515-03-7	73.92	1.54	34.75	1.97	60.13	2.24	38.75	2.58	44.07	1.60
carbonyls	aromatics	Benzaldehyde	100-52-7	19.25	0.84	6.21	1.76	10.53	2.00	9.08	2.64	14.60	1.42
	terpenoid	Carvone	99-49-0 / 6485-40-1 / 2244-16-8	32.21	1.15	13.55	1.90	23.27	2.16	17.50	1.87	19.53	1.84
	aromatics	Cinnamal	104-55-2	33.50	1.61	14.25	2.31	24.00	2.61	17.92	3.76	25.73	1.40
	nor isoprenoid	Damascenone	23696-85-7	38.34	0.98	16.96	1.73	29.67	1.98	21.42	1.45	21.60	2.07
	nor isoprenoid	δ-Damascone	57378-68-4	38.75	0.98	17.21	1.83	29.93	2.05	21.58	1.56	22.20	2.50
	nor-isoprenoid	α -Damascone (Z)	43052-87-5 / 23726-94-5	39.13	0.98	17.46	1.76	30.40	2.01	22.42	1.46	20.40	2.22
	aromatics	Vanillin	121-33-5	39.34	2.03	17.67	2.56	29.53	3.10	21.92	3.94	32.80	1.24
	nor isoprenoid	β-Damascone (Z)	23726-92-3	40.13	1.01	18.00	1.83	31.33	2.04	23.42	1.47	21.53	2.26
	aromatics	Coumarin	91-64-5	41.63	2.06	18.59	0.35	31.13	3.09	22.50	0.72	30.20	1.18
	aromatics	6-Methylcoumarine	92-48-8	46.96	1.96	21.46	2.69	36.40	2.98	25.58	4.83	33.00	1.33
	aromatics	Amyl Cinnamal	122-40-7	50.09	1.12	23.55	1.93	41.07	2.14	28.08	1.88	30.07	1.79
	aromatics	Hexil Cinnamal (E)	101-86-0	54.13	1.01	25.71	1.90	44.20	2.11	30.75	1.75	31.87	1.83
esters	terpenoid	Linalyl Acetate	115-95-7	32.13	0.66	13.84	1.49	22.93	1.97	18.00	1.26	15.80	2.30
	terpenoid	Geranyl Acetate	105-87-3	37.96	0.73	17.21	1.62	24.27	1.78	17.83	2.22	20.33	2.07
	aromatics	Eugenyl Acetate	93-28-7	44.63	1.22	20.80	2.21	35.93	2.46	24.67	2.65	24.00	1.55
	aromatics	Isoeugenyl Acetate	93-29-8	48.42	1.29	22.84	2.25	38.60	2.42	26.83	2.90	30.00	1.51
	aromatics	Benzyl Benzoate	120-51-4	55.13	1.12	26.09	2.38	44.53	2.26	31.00	2.71	36.13	1.46
	aromatics	Benzyl Salicylate	118-58-1	59.38	1.08	27.88	1.93	48.27	1.94	34.17	2.61	44.67	1.35
	hydrocarbon	Hexadecanolactone	109-29-5	62.30	0.84	29.42	1.80	51.27	1.97	31.50	1.68	32.13	2.45
hydrocarbon	terpenoid	α -Pinene	80-56-8	18.21	2.69	5.63	1.11	10.67	1.41	9.17	0.99	5.20	2.02
	terpenoid	β-Pinene	127-91-3	20.09	0.31	6.55	1.21	12.27	1.49	10.33	1.04	6.20	2.22
	terpenoid	Limonene	138-86-3	22.05	0.35	7.80	1.28	14.40	1.53	11.75	1.08	7.67	2.31
	terpenoid	Terpinolene	586-62-9	24.75	0.42	9.30	1.42	16.93	1.58	13.50	1.13	9.33	2.40
	terpenoid	Camphor	76-22-2 / 464-49-3	27.80	1.05	10.80	1.87	19.00	2.09	14.83	1.53	14.53	2.23
	terpenoid	β-Caryophillene	87-44-5	40.88	0.70	18.09	1.52	32.53	1.71	23.25	1.11	16.87	3.28
	aromatics	Anethole	4180-23-8	34.05	0.94	14.63	1.93	26.93	1.99	18.75	1.98	21.67	1.61

1 Table 2

	Column(s) and restrictors	Carrier gas (He)[a] settings	Modulation settings	Oven programming
Set-up I	^{1}D: SE52[b] (30 m, 0.25 mm d_c, 0.25 µm d_f) ^{2}D: OV1701[c] (5 m, 0.25 mm d_c, 0.25 µm d_f) Restrictor to monitor FID: deactivated 0.8 m, 0.05 mm d_c Splitter for MS/FID dual detection: deactivated capillary to MS detector: 0.17 m, 0.1 mm d_c deactivated capillary to FID detector: 1.3 m, 0.45 mm d_c	^{1}D p_i: 270.0 KPa - $^{1}\bar{u}$: 5.1 cm/s - 0.35 mL/min hold-up: 5.8 min p_2: 252.6 KPa - $^{2}\bar{u}$: 472 cm/s - 27 mL/min hold-up: 1.2 s split ratio (MS/FID): 25:75	Modulation period 2.5 s Injection time: 0.11 s	VMM mixture, *n*-alkanes (C9-C25) 80°C (2 min) to 280°C (10 min) @ 3°C/min
Set-up II	^{1}D: SE52[b] (10 m, 0.10 mm d_c, 0.10 µm d_f) parallel ^{2}D: OV1701[c] 2×(1.0 m, 0.10 mm d_c, 0.10 µm d_f) Restrictor to monitor FID: deactivated 10.0 m, 0.05 mm d_c Splitter for MS/FID dual parallel: deactivated capillary: 0.1 m, 0.1 mm d_c	^{1}D p_i: 436 KPa - $^{1}\bar{u}$: 22.8 cm/s - 0.40 mL/min hold-up: 0.73 min p_2: 334 KPa - $^{2}\bar{u}_{MS}$: 494 cm/s - 6.1 mL/min p_2: 334 KPa - $^{2}\bar{u}_{FID}$: 447 cm/s - 5.8 mL/min hold-up: 0.22 s - split ratio MS/FID 51:49	Modulation period 2.5 s Injection time: 0.11 s	VMM mixture, *n*-alkanes (C9-C25) 50°C (1 min) to 280°C (10 min) @ 5°C/min
Set-up III	^{1}D: OV1[d] (10 m, 0.10 mm d_c, 0.40 µm d_f) parallel ^{2}D: OV1701[c] 2×(1.5 m, 0.10 mm d_c, 0.10 µm d_f) Restrictor to monitor FID: deactivated 10.0 m, 0.05 mm d_c Splitter for MS/FID dual parallel: deactivated capillary: 0.1 m, 0.1 mm d_c	^{1}D p_i: 387 KPa - $^{1}\bar{u}$: 22.8 cm/s - 0.40 mL/min hold-up: 0.73 min p_2: 334 KPa - $^{2}\bar{u}_{MS}$: 329 cm/s - 4.1 mL/min p_2: 334 KPa - $^{2}\bar{u}_{FID}$: 298 cm/s - 3.9 mL/min hold-up: 0.6 s - split ratio MS/FID 51:49	Modulation period 4.0 s Injection time: 0.11 s	VMM mixture, *n*-alkanes (C9-C25) 50°C (1 min) to 280°C (10 min) @ 3°C/min
Set-up IV	^{1}D: OV1[d] (10 m, 0.10 mm d_c, 0.40 µm d_f) parallel ^{2}D: PEG[e] 2×(1.5 m, 0.10 mm d_c, 0.10 µm d_f) Restrictor to monitor FID: deactivated 10.0 m, 0.05 mm d_c Splitter for MS/FID dual parallel: deactivated capillary: 0.1 m, 0.1 mm d_c	^{1}D p_i: 436 KPa - $^{1}\bar{u}$: 22.8 cm/s - 0.40 mL/min hold-up: 0.73 min p_2: 357 KPa - $^{2}\bar{u}_{MS}$: 333 cm/s - 4.1 mL/min p_2: 357 KPa - $^{2}\bar{u}_{FID}$: 304 cm/s - 3.9 mL/min hold-up: 0.6 s - split ratio MS/FID 51:49	Modulation period 4.0 s and 5.0 s Injection time: 0.11 s	VMM mixture, *n*-alkanes (C9-C25), Mint and Lavender EOs 70°C (1 min) to 280°C (10 min) @ 5°C/min Vetiver EOs 120°C (2 min) to 280°C (10 min) @ 2.5°C/min
Set-up V	^{1}D: PEG[e] (10 m, 0.10 mm d_c, 0.10 µm d_f) parallel ^{2}D: OV1701[c] 2×(1.5 m, 0.10 mm d_c, 0.10 µm d_f) Restrictor to monitor FID: deactivated 10.0 m, 0.05 mm d_c Splitter for MS/FID dual parallel: deactivated capillary: 0.1 m, 0.1 mm d_c	^{1}D p_i: 387 KPa - $^{1}\bar{u}$: 22.8 cm/s - 0.40 mL/min hold-up: 0.73 min p_2: 334 KPa - $^{2}\bar{u}_{MS}$: 329 cm/s - 4.1 mL/min p_2: 334 KPa - $^{2}\bar{u}_{FID}$: 298 cm/s - 3.9 mL/min hold-up: 0.6 s - split ratio MS/FID 51:49	Modulation period 4.0 s Injection time: 0.11 s	VMM mixture, *n*-alkanes (C9-C25), Mint and Lavender EOs 50°C (1 min) to 250°C (10 min) @ 5°C/min

[a]: reported values were calculated on the basis of reference equations and are just approximations of real ones
[b]: SE52 (95% polydimethylsiloxane, 5% phenyl)
[c]: OV1701 (86% polydimethylsiloxane, 7% phenyl, 7% cyanopropyl)
[d]: OV1 (100% polydimethylsiloxane)
[e]: PEG (100% polyethylene glycol)

2

3

Table 3

Set-up	Re-injection pulse width ($^2\sigma_i$) ms	First Peak	^{1}D Rt s	^{1}D σ	^{2}D σ	M_R	Last Peak	^{1}D Rt s	^{1}D σ	^{2}D σ	M_R	S_1	Exp S_2	S_{GCxGC}	S_{GCxGC}/t_A	Separation space used	% of usage	Area total (pixel)	Area used (pixel)	Ratio
I	45	α-pinene	1093	3.93	0.05	6.29	sclareol	4435	8.74	0.11	13.98	528	17	8711	2.0	0.66	66	83160	41445	0.50
II	90	α-pinene	340	2.28	0.06	3.65	sclareol	2085	5.08	0.10	8.13	474	29	13512	6.5	0.95	95	176700	75369	0.43
III	90	α-pinene	640	4.19	0.11	4.19	sclareol	3608	3.96	0.07	3.96	728	38	27466	7.6	0.74	74	215670	70581	0.33
IV	75	α-pinene	550	4.24	0.10	4.24	sclareol	2445	3.36	0.10	3.36	499	34	16955	6.9	0.98	98	170100	106322	0.63
V	75	α-pinene	240	2.41	0.07	2.41	benzyl salicilate	2680	3.91	0.08	3.91	772	46	35724	13.3	0.75	75	195274	79089	0.41

10 Table 4

		Set-up I				Set-up II				Set-up III				Set-up IV				Set-up V			
		Symmetry		Peak variances		Symmetry		Peak variances		Symmetry		Peak variances		Symmetry		Peak variances		Symmetry		Peak variances	
	Compound name	**^{1}D**	**^{2}D**	**^{1}D**	**^{2}D**	**^{1}D**	**^{2}D**	**^{1}D**	**^{2}D**	**^{1}D**	**^{2}D**	**^{1}D**	**^{2}D**	**^{1}D**	**^{2}D**	**^{1}D**	**^{2}D**	**^{1}D**	**^{2}D**	**^{1}D**	**^{2}D**
hydrocarbons	α-Pinene	1.40	12.38	4.29E-03	2.19E-03	1.9	1.9	2.72E-03	3.85E-03	2.14	0.63	4.88E-03	1.14E-03	1.0	3.9	5.00E-03	1.41E-02	1.44	2.72	2.63E-03	5.17E-03
	β-Pinene	1.31	1.62	3.97E-03	2.90E-03	2.4	1.0	2.98E-03	4.47E-03	1.44	2.57	2.51E-03	6.50E-03	2.1	3.5	9.39E-03	1.18E-02	3.00	3.76	5.85E-04	4.70E-03
	Limonene	1.00	1.24	3.98E-03	3.37E-03	1.9	2.0	4.15E-03	1.03E-02	1.86	3.74	3.77E-03	5.72E-03	2.1	4.4	6.26E-03	2.64E-02	3.40	2.95	3.73E-03	6.01E-03
	Terpinolene	1.13	0.91	4.44E-03	5.03E-03	1.9	3.6	2.72E-03	1.31E-02	2.33	0.91	4.90E-03	2.36E-03	2.1	1.3	9.10E-03	4.26E-03	3.40	2.78	2.40E-03	6.42E-03
	Camphor	1.46	0.84	4.90E-03	6.89E-03	4.2	0.9	6.14E-03	9.51E-03	2.43	10.47	5.19E-03	1.05E-02	7.0	0.8	8.06E-03	3.61E-03	1.44	2.52	3.77E-03	4.67E-03
	β-Caryophyllene	1.00	1.71	4.41E-03	7.18E-03	1.7	0.5	4.56E-03	3.19E-03	0.85	0.83	3.93E-03	1.80E-03	6.3	1.7	7.16E-03	3.20E-03	0.69	1.84	2.87E-03	5.87E-03
	Mean	***1.22***	***3.12***	***4.33E-03***	***4.59E-03***	***2.33***	***1.65***	***3.88E-03***	***7.41E-03***	***1.84***	***3.19***	***4.20E-03***	***4.67E-03***	***3.46***	***2.59***	***7.49E-03***	***1.06E-02***	***2.23***	***2.76***	***2.66E-03***	***5.48E-03***
esters	Linalyl acetate	1.55	0.85	4.23E-03	3.70E-03	3.4	0.3	3.72E-03	2.27E-03	2.71	2.51	6.48E-03	1.25E-02	1.3	2.4	3.83E-03	6.11E-03	1.22	2.41	4.66E-03	5.03E-03
	Geranyl acetate	0.87	1.29	4.74E-03	8.65E-03	2.2	0.3	2.53E-03	2.67E-03	1.73	0.84	4.69E-03	2.23E-03	3.7	3.1	5.38E-03	1.78E-02	1.55	1.11	4.21E-03	1.37E-03
	Eugenyl acetate	0.65	2.82	5.05E-03	1.71E-02	2.5	3.9	6.74E-03	1.77E-02	1.00	1.71	4.58E-03	3.18E-03	1.0	4.1	5.32E-03	4.69E-03	0.73	2.24	3.73E-03	2.77E-03
	Isoeugenyl acetate	1.00	1.94	6.48E-03	2.26E-02	2.1	1.3	5.57E-03	2.09E-02	2.54	3.40	1.66E-02	1.41E-02	1.7	2.1	6.57E-03	1.79E-02	0.82	2.33	1.89E-03	2.11E-03
	Benzyl benzoate	1.13	1.59	6.54E-03	1.73E-02	1.4	2.4	4.30E-03	2.24E-02	2.14	5.00	8.23E-03	8.60E-03	6.3	1.8	1.10E-02	1.14E-02	3.00	7.24	1.07E-02	6.30E-03
	Benzyl salicylate	1.46	1.11	1.36E-02	1.49E-02	1.7	2.1	4.11E-03	1.30E-02	1.00	1.34	4.97E-03	2.59E-03	2.1	2.6	1.19E-02	1.68E-02	1.00	3.64	4.25E-03	5.92E-03
	Hexadecanolactone	1.11	2.73	1.27E-02	4.57E-02	1.6	3.2	3.94E-03	3.63E-02	1.91	3.90	4.01E-03	4.85E-03	2.2	1.3	1.17E-02	4.33E-03	0.60	4.04	1.64E-03	4.90E-03
	Mean	***1.11***	***1.76***	***7.62E-03***	***1.86E-02***	***2.12***	***1.93***	***4.41E-03***	***1.65E-02***	***1.86***	***2.67***	***7.09E-03***	***6.86E-03***	***2.61***	***2.48***	***7.95E-03***	***1.13E-02***	***1.27***	***3.29***	***4.44E-03***	***4.06E-03***
carbonyls	Benzaldehyde	1.42	2.09	8.46E-03	7.25E-03	1.9	2.7	2.82E-03	2.01E-02	3.44	2.78	2.74E-02	1.22E-02	3.4	2.3	6.00E-03	1.84E-02	2.11	2.72	1.08E-02	5.43E-03
	Carvone	1.46	2.85	6.24E-03	2.24E-02	1.2	4.4	3.80E-03	1.43E-02	2.43	4.28	6.59E-03	1.28E-02	0.8	2.6	4.73E-03	5.95E-03	1.15	0.48	5.78E-03	6.38E-04
	Cinnamaldehyde	0.38	1.24	4.04E-03	1.48E-02	1.4	3.2	4.97E-03	4.16E-02	1.18	3.60	1.03E-02	2.74E-02	1.3	1.7	6.60E-03	3.07E-02	3.00	2.03	3.31E-02	4.90E-03
	β-Damascenone	0.85	2.47	3.60E-03	1.67E-02	1.0	2.1	1.83E-03	1.05E-02	0.60	13.46	5.03E-03	1.53E-02	3.0	2.2	5.16E-03	2.40E-03	1.00	0.85	1.91E-03	1.74E-03
	δ-Damascone	1.18	1.24	4.37E-03	7.06E-03	1.4	3.7	2.04E-03	1.17E-02	1.80	3.56	4.88E-03	4.57E-03	0.6	4.6	5.45E-03	1.58E-02	0.69	2.30	2.32E-03	4.37E-03
	α-Damascone (*Z*)	1.44	1.42	3.76E-03	1.07E-02	3.8	1.7	5.66E-03	1.42E-02	2.60	3.29	3.87E-03	4.70E-03	1.9	3.3	5.86E-03	1.43E-02	0.85	6.08	5.66E-03	4.98E-03
	Vanillin	1.35	1.29	1.64E-02	2.84E-02	1.6	1.7	4.64E-03	2.31E-02	1.77	3.42	2.39E-02	4.67E-02	1.7	1.4	4.38E-03	1.52E-02	1.55	1.94	2.01E-02	1.96E-03
	β-Damascone (*E*)	1.00	1.00	3.80E-03	4.75E-03	3.3	3.5	4.89E-03	1.98E-02	1.73	3.97	3.75E-03	5.51E-03	4.3	3.1	3.79E-03	9.91E-03	1.36	6.18	2.54E-03	5.08E-03
	Coumarine	1.77	1.19	1.03E-02	2.42E-02	1.4	2.1	5.30E-03	4.64E-02	1.77	3.04	3.08E-02	3.13E-02	1.2	1.6	1.20E-02	3.04E-02	0.60	3.00	8.78E-04	3.75E-03
	6-Methyl coumarine	0.89	2.05	9.92E-03	4.43E-02	1.2	2.0	4.05E-03	6.48E-02	1.46	3.93	2.39E-02	3.39E-02	1.6	1.5	5.54E-03	1.99E-02	6.43	1.19	6.81E-02	1.73E-03
	Amyl cinnamic aldehyde	0.85	1.27	4.44E-03	1.26E-02	1.0	2.1	2.14E-03	1.68E-02	1.36	1.09	5.34E-03	3.31E-03	1.2	2.3	5.04E-03	9.19E-03	0.64	3.09	2.35E-03	3.61E-03
	Hexyl cinnamaldehyde	1.13	2.33	6.99E-03	3.24E-02	1.4	3.8	2.50E-03	4.84E-02	2.11	2.47	8.93E-03	5.85E-03	3.0	2.9	7.60E-03	9.32E-03	2.43	3.82	3.56E-03	3.40E-03
	Mean	***1.14***	***1.70***	***6.86E-03***	***1.88E-02***	***1.72***	***2.73***	***3.72E-03***	***2.77E-02***	***1.85***	***4.07***	***1.29E-02***	***1.70E-02***	***2.00***	***2.43***	***6.02E-03***	***1.51E-02***	***1.82***	***2.81***	***1.31E-02***	***3.47E-03***
alcohols	Benzyl Alcohol	1.12	2.54	7.86E-03	2.54E-02	7.0	3.5	5.32E-03	3.28E-02	1.00	1.44	5.42E-03	3.30E-03	5.0	5.7	7.41E-03	6.58E-02	3.14	1.59	6.39E-02	2.70E-03
	Linalool	1.12	2.38	4.85E-03	1.07E-02	2.1	2.5	3.60E-03	2.27E-02	1.13	4.84	5.78E-03	1.62E-02	1.7	2.8	5.55E-03	1.11E-02	1.36	3.44	2.84E-03	4.83E-03
	Menthol	1.00	2.07	4.89E-03	1.36E-02	1.9	2.7	3.96E-03	2.72E-02	1.44	3.86	5.72E-03	9.47E-03	2.3	2.0	9.63E-03	1.47E-02	1.06	6.65	6.42E-03	7.95E-03
	α-Terpineol	0.60	1.95	4.44E-03	1.52E-02	0.6	1.0	1.52E-03	4.06E-03	0.71	2.68	3.79E-03	6.20E-03	5.7	6.3	7.85E-03	4.91E-02	1.00	5.00	6.57E-03	5.55E-03
	Citronellol	1.73	1.77	8.11E-03	1.41E-02	1.9	2.2	2.76E-03	1.98E-02	3.80	2.33	9.61E-03	7.24E-03	3.0	0.6	6.98E-03	2.84E-03	1.89	1.38	1.53E-02	3.51E-03
	Cinnamyl Alcohol	1.00	1.35	1.07E-02	1.69E-02	3.0	2.6	7.75E-03	2.48E-02	2.43	1.97	6.19E-03	4.15E-03	1.9	1.4	9.12E-03	4.01E-02	1.67	3.80	8.45E-02	5.27E-03

Eugenol	1.13	1.80	8.67E-03	2.04E-02	1.4	1.5	4.08E-03	3.47E-02	2.27	3.51	1.31E-02	1.54E-02	3.0	2.9	4.81E-03	4.77E-02	1.89	2.82	1.71E-02	7.08E-03
Isoeugenol	1.10	2.09	1.73E-02	1.90E-02	3.0	3.9	8.23E-03	5.24E-02	1.00	2.52	9.00E-03	9.22E-03	1.9	1.6	5.61E-03	3.19E-02	3.00	2.88	1.61E-02	3.53E-03
(Z)-α-Santalol	2.82	4.56	2.73E-02	2.31E-02	2.6	1.6	4.19E-03	2.23E-02	1.29	3.10	4.57E-03	5.68E-03	0.6	2.0	1.04E-02	1.17E-02	0.71	4.37	2.23E-03	5.36E-03
(*E,Z*)-Farnesol	0.28	0.14	2.85E-02	1.12E-03	3.4	2.2	6.36E-03	3.62E-02	3.00	1.00	5.65E-03	3.80E-03	1.0	1.5	9.00E-03	3.74E-03	0.71	3.52	2.93E-03	7.01E-03
(*Z*)-β-Santalol	1.31	4.20	1.05E-02	1.13E-02	3.6	3.2	1.14E-02	2.06E-02	1.44	19.29	5.99E-03	1.03E-02	2.3	2.0	4.75E-03	4.81E-03	2.60	0.70	1.21E-02	1.90E-03
(*E,E*)-Farnesol	1.00	0.37	7.65E-03	6.42E-03	2.3	0.1	1.66E-02	4.42E-03	2.43	0.33	5.65E-03	1.43E-03	2.2	1.2	7.93E-03	3.71E-03	0.60	1.63	2.53E-03	1.75E-03
Sclareol	1.11	1.00	2.12E-02	1.23E-02	1.5	1.1	7.18E-03	1.26E-02	1.46	3.71	4.36E-03	5.24E-03	0.1	2.9	3.13E-03	9.09E-03	1.55	3.35	1.82E-02	3.92E-03
Mean	***1.18***	***2.02***	***1.25E-02***	***1.46E-02***	***2.64***	***2.16***	***6.38E-03***	***2.42E-02***	***1.80***	***3.89***	***6.52E-03***	***7.51E-03***	***2.36***	***2.53***	***7.09E-03***	***2.28E-02***	***2.59***	***3.16***	***1.93E-02***	***4.64E-03***
Anethole	2.27	1.32	6.58E-03	7.62E-03	0.7	0.7	1.65E-03	7.49E-03	1.89	1.42	4.23E-03	4.91E-03	0.8	1.9	3.59E-03	9.64E-03	0.60	2.31	7.81E-03	4.36E-03

11

12 Table 5

							Mentha x *piperita L.*								*Mentha spicata* L.			
Analyte	**MW**	**Formula**	**1D Rt (min)**	**CV%**	**2D Rt (s)**	**CV%**	**Norm. 2D Vol**	**CV%**	**2D Vol %**	**Amount (g/100g) FID-PRF**	**Amount (g/100g) ESTD**	**Rec. %***	**Norm. 2D Vol**	**CV%**	**2D Vol %**	**Amount (g/100g) FID-PRF**	**Amount (g/100g) ESTD**	**Rec. %***
α-Pinene	136	C10H16	3.80	0.00	1.84	0.54	1.48	3.23	1.03	0.79			1.35	4.74	1.24	0.96		
β-Pinene	136	C10H16	5.00	0.00	2.05	0.28	1.72	4.09	1.19	0.91			0.37	11.78	0.34	0.26		
Sabinene	136	C10H16	5.20	0.00	2.00	0.29	1.30	4.10	0.90	0.69			0.57	3.31	0.53	0.41		
α-Terpinene	136	C10H16	6.00	0.00	1.93	0.30	0.32	9.12	0.22	0.17			0.42	3.13	0.39	0.30		
Myrcene	136	C10H16	6.27	0.00	2.14	0.27	0.32	9.63	0.22	0.17			0.00	6.68	0.00	0.00		
Limonene	136	C10H16	6.67	0.00	2.09	0.28	2.10	6.61	1.46	1.12	1.05	106	10.56	4.58	9.69	7.50	7.04	106
1,8-Cineole	154	C10H18O	6.87	0.00	2.27	0.25	9.30	7.57	6.46	5.62	5.56	101	0.96	3.96	0.88	0.77	0.64	121
γ-Terpinene	136	C10H16	7.60	0.00	2.15	0.47	0.31	7.21	0.22	0.17			0.03	3.01	0.03	0.02		
p-Cymene	136	C10H16	8.13	0.00	1.82	0.32	0.58	0.77	0.40	0.28			0.07	9.21	0.06	0.04		
3-Octyl acetate	172	C10H20O2	8.93	0.00	2.66	0.22	0.11	1.77	0.08	0.08			0.10	7.17	0.09	0.09		
3-Octanol	130	C8H18O	11.00	0.00	1.24	0.47	0.32	2.61	0.22	0.19			1.43	8.40	1.31	1.16		
cis-Sabinenehydrate	154	C10H18O	12.67	0.00	1.39	0.41	1.76	5.79	1.22	1.06			0.12	1.52	0.11	0.10		
Menthone	154	C10H18O	12.73	0.00	2.16	0.00	23.32	5.02	16.20	14.11			1.04	0.59	0.95	0.84		
1-Octen-3-ol	128	C8H16O	12.80	0.00	1.08	4.90	0.04	2.76	0.03	0.02			-	-	-	-		
Menthofuran	150	C10H14O	13.11	0.29	1.77	0.65	2.55	1.95	1.77	1.61	1.67	97	-	-	-	-		
Isomenthone	154	C10H18O	13.27	0.00	2.14	0.27	3.91	4.92	2.71	2.36			0.14	3.63	0.13	0.11		
β-Bourbonene	204	C15H24	14.27	0.00	3.49	0.00	0.63	4.80	0.44	0.33			0.93	3.04	0.85	0.65		
Neomenthyl acetate	198	C12H22O2	14.36	0.27	2.54	0.39	0.30	4.42	0.21	0.20			-	-	-	-		
n-Pentadecane (ISTD)	212	C15H32	14.67	0.00	0.96	1.04	1.00	0.00	0.69	0.50			1.00	0.00	0.92	0.67		
Linalool	154	C10H18O	14.67	0.00	1.18	0.49	1.16	3.93	0.81	0.70	0.68	103	0.09	7.28	0.08	0.07	0.06	121
Isopulegol	154	C10H18O	15.07	0.00	1.80	0.00	0.10	4.02	0.07	0.06			0.02	4.05	0.02	-		
Menthyl acetate	198	C12H22O2	15.20	0.00	2.34	0.25	6.85	3.59	4.76	4.49	5.40	83	-	-	-	0.01		
Isopulegone	154	C10H18O	15.33	0.00	1.79	0.32	0.06	6.12	0.04	0.04	0.03	132	-	-	-	-		
Isomenthyl acetate	198	C12H22O2	15.53	0.00	2.48	0.23	0.43	4.52	0.30	0.28			-	-	-	-		
Terpinen-4-ol	154	C10H18O	15.87	0.00	1.35	0.43	2.10	1.67	1.46	1.27	1.22	104	0.13	2.67	0.12	-		
Neomenthol	156	C10H20O	15.87	0.00	1.45	6.58	3.84	6.13	2.67	2.28	1.87	122	-	-	-	0.11	0.09	121
β-Elemene	204	C15H24	15.98	0.24	2.78	0.62	0.30	3.47	0.21	0.16			0.17	3.65	0.16	-		
trans-β-Caryophyllene	204	C15H24	16.07	0.00	3.15	0.18	3.85	4.18	2.67	2.01			0.30	7.20	0.27	0.12		
trans-Dihydrocarvone	152	C10H16O	16.16	3.10	1.76	2.05	-	-	-	-			0.93	2.60	0.85	0.21		
Neoisomenthol	156	C10H20O	16.53	0.00	1.36	0.43	0.99	1.24	0.69	0.59	0.48	121	-	-	-	0.76		
Pulegone	152	C10H16O	16.80	0.00	1.76	0.33	2.27	2.73	1.58	1.40	1.25	112	-	-	-	-		
Menthol	156	C10H20O	17.07	0.00	1.23	0.47	66.55	6.35	46.22	39.46	38.43	103	0.16	1.64	0.15	-		
α-Terpineol	154	C10H18O	17.47	0.00	1.20	0.48	0.76	2.28	0.53	0.46			0.43	4.81	0.40	0.13	0.11	119
trans-Dihydrocarvyl acetate	196	C12H20O2	17.67	0.00	1.92	0.30	-	-	-	-			0.58	9.76	0.53	0.35		
trans-β-Farnesene	204	C15H24	17.67	0.00	2.86	0.20	0.52	1.94	0.36	0.27			0.11	6.64	0.10	0.50		

Germacrene D	204	C15H24	18.47	0.00	2.81	0.21	0.91	7.38	0.63	0.47	0.06	10.70	0.05	0.08		
Piperitone	152	C10H16O	18.53	0.00	1.62	0.36	0.91	0.70	0.64	0.56	-	-	-	0.04		
Dihydrocarveol	154	C10H18O	18.87	0.00	1.10	0.91	-	-	-	-	0.30	8.47	0.28	-		
Carvone	150	C10H14O	19.04	0.20	1.38	0.00	-	-	-	-	85.33	1.44	78.28	0.25		
δ-Cadinene	204	C15H24	19.53	0.00	2.58	0.22	0.16	2.15	0.11	0.08	0.09	11.16	0.08	71.80	56.89	126
cis-Dihydrocarvyl acetate	196	C12H20O2	19.67	0.00	1.65	0.35	-	-	-	-	0.21	0.45	0.19	0.06		
trans-Carveol	152	C10H16O	20.93	0.00	0.97	0.00	-	-	-	-	0.50	1.56	0.46	0.18		
cis-Carveol	152	C10H16O	21.53	0.00	0.95	1.05	-	-	-	-	0.46	6.39	0.43	0.41		
Caryophyllene oxide	220	C15H24O	23.89	0.16	2.31	0.43	0.13	8.76	0.09	0.08	0.69	3.78	0.63	0.38		
Viridiflorol	222	C15H26O	25.93	0.00	1.67	0.35	0.87	4.31	0.60	0.49	0.11	2.11	0.10	0.53		
Spathulenol	220	C15H24O	26.62	0.14	1.51	0.38	0.11	4.42	0.08	0.07	-	-	-	0.08		

*: the bias is expressed as Recovery % was calculated by dividing the FID PRF estimated amount by the resulting amount from external calibration with reference standards

13

14

15 Table 6

			Lavandula angustifolia Mill. x *Lavandula latifolia* Medik Lavandin "grosso"										*Lavandula angustifolia* Mill. Lavender					
Analyte	**MW**	**Formula**	**1D Rt (min)**	**CV%**	**2D Rt (s)**	**CV%**	**Norm. 2D Vol**	**CV%**	**2D Vol %**	**Amount (g/100g) FID-PRF**	**Amount (g/100g) ESTD**	**Rec. %***	**Norm. 2D Vol**	**CV%**	**2D Vol %**	**Amount (g/100g) FID-PRF**	**Amount (g/100g) ESTD**	**Rec. %***
α-Pinene	136	C10H16	3.80	0.00	1.85	0.22	0.87	9.41	1.05	0.93			0.35	7.85	0.42	0.37		
Camphene	136	C10H16	4.33	0.00	1.93	0.21	0.23	9.12	0.28	0.25			0.15	13.36	0.18	0.16		
β-Pinene	136	C10H16	5.00	0.00	2.07	0.20	0.36	7.85	0.43	0.38			0.06	7.17	0.07	0.06		
Sabinene	136	C10H16	5.67	0.00	2.18	0.24	0.07	10.95	0.08	0.07			0.10	9.73	0.12	0.11		
Myrcene	136	C10H16	6.02	0.57	1.91	0.54	1.75	2.65	2.11	1.87			1.60	7.07	1.90	1.70		
Limonene	136	C10H16	6.67	0.00	2.10	0.25	0.74	5.47	0.89	0.79	0.74	106	0.40	2.29	0.47	0.43	0.40	106
1,8-Cineole	154	C10H18O	6.98	4.39	2.25	2.08	7.38	4.29	8.90	8.93	8.85	101	2.24	6.27	2.66	2.71	2.73	99
Hexyl propanoate	158	C9H18O	7.03	0.52	2.01	0.54	0.05	6.24	0.06	0.07			0.07	7.82	0.08	0.09		
δ-3-Carene	136	C10H16	7.47	0.00	1.96	0.38	0.29	4.24	0.35	0.31			0.38	4.17	0.45	0.40		
cis-β-Ocimene	136	C10H16	7.83	0.47	1.98	0.76	0.91	6.80	1.10	0.97			2.38	5.16	2.83	2.54		
trans-β-Ocimene	136	C10H16	8.13	0.00	1.82	0.45	0.32	5.74	0.38	0.34			0.48	2.55	0.57	0.51		
Hexyl acetate	144	C8H16O2	8.37	4.12	1.79	3.13	0.01	6.38	0.01	0.01			0.00	6.07	0.00	0.01		
Hexanol	102	C6H14O	9.93	0.00	0.90	0.91	0.10	6.63	0.12	0.14			0.08	10.78	0.10	0.12		
Octen-1-ol acetate	170	C10H18O2	10.80	0.00	1.99	0.55	0.22	11.76	0.27	0.31			0.78	8.30	0.92	1.08		
Hexyl butanoate	172	C10H20O2	11.79	1.15	2.52	0.25	0.26	4.08	0.31	0.35			0.18	5.27	0.21	0.24		
trans Linalool oxide	170	C10H18O2	12.04	0.45	1.51	0.36	0.12	10.94	0.14	0.16			0.16	5.10	0.19	0.22		
1-Octen-3-ol	128	C8H16O	12.33	0.00	1.01	0.98	0.17	8.44	0.20	0.21			0.21	2.78	0.25	0.27		
trans-Sabinene hydrate	154	C10H18O	12.60	0.00	1.43	0.29	0.12	2.26	0.14	0.14			0.03	1.45	0.04	0.04		
cis Linalool oxide	170	C10H18O2	12.73	0.00	1.49	0.51	0.10	9.77	0.12	0.13			0.10	7.54	0.12	0.14		
Camphor	152	C10H16O	13.70	0.27	1.89	0.43	7.43	2.50	8.95	9.17	8.30	110	1.36	6.32	1.62	1.68	1.60	105
Linalool	154	C10H18O	14.87	0.00	1.14	0.45	20.23	2.77	24.37	24.47	21.64	113	23.31	3.36	27.68	28.19	24.92	113
Linalyl acetate	196	C12H20O2	15.02	1.60	0.74	1.01	24.32	4.87	29.30	32.39	36.78	88	36.56	2.58	43.42	48.69	55.33	88
n-Pentadecane (ISTD)	212	C15H32	15.30	0.24	1.90	0.70	1.00	0.00	1.20	1.00			1.00	0.00	1.19	1.00		
α-Santalene	204	C15H24	15.61	0.17	3.14	0.33	0.48	4.39	0.58	0.51			0.31	2.81	0.37	0.33		
4-Terpineol	154	C10H18O	15.93	0.00	1.38	0.00	3.57	7.79	4.30	4.31	3.56	121	2.08	2.44	2.47	2.51	2.07	121
trans Caryophyllene	204	C15H24	16.03	0.51	3.16	0.83	1.63	5.60	1.97	1.71			0.09	8.97	0.11	0.09		
Lavandulyl acetate	196	C12H20O2	16.27	0.00	1.92	0.27	2.64	8.04	3.18	3.52	3.94	89	2.92	3.81	3.47	3.89	4.36	89
Lavandulol	154	C10H18O	17.67	0.00	1.10	0.68	0.53	4.22	0.63	0.64	0.52	122	0.58	3.50	0.69	0.70	0.58	122
trans-ß-Farnesene	204	C15H24	17.73	0.00	2.60	0.34	0.97	5.34	1.17	1.02			0.60	3.97	0.71	0.62		
α-Terpineol	154	C10H18O	18.00	0.00	1.17	0.44	2.08	6.07	2.51	2.52			1.38	6.22	1.64	1.67		
Borneol	154	C10H18O	18.07	0.00	1.13	0.36	1.83	1.55	2.20	2.21	1.82	121	1.12	9.09	1.33	1.35	1.11	122
Neryl Acetate	196	C12H20O2	18.81	0.14	1.78	0.59	0.57	0.69	0.69	0.76			0.64	8.11	0.76	0.86		
Geranyl acetate	196	C12H20O2	19.53	0.00	1.72	0.48	1.11	10.91	1.34	1.48			1.55	9.58	1.84	2.06		
p-Cymen-8-ol	150	C10H14O	21.11	0.16	0.89	1.00	0.10	1.22	0.12	0.13			0.17	5.17	0.21	0.22		
Geraniol	154	C10H18O	21.27	0.00	0.99	0.90	0.37	3.51	0.45	0.45			0.43	2.68	0.50	0.51		
Caryophyllene oxide	220	C15H24O	23.91	0.14	2.29	0.86	0.08	3.20	0.10	0.10			0.35	10.28	0.42	0.41		

*: the bias is expressed as Recovery % was calculated by dividing the FID PRF estimated amount by the resulting amount from external calibration with reference standards

Figure 1

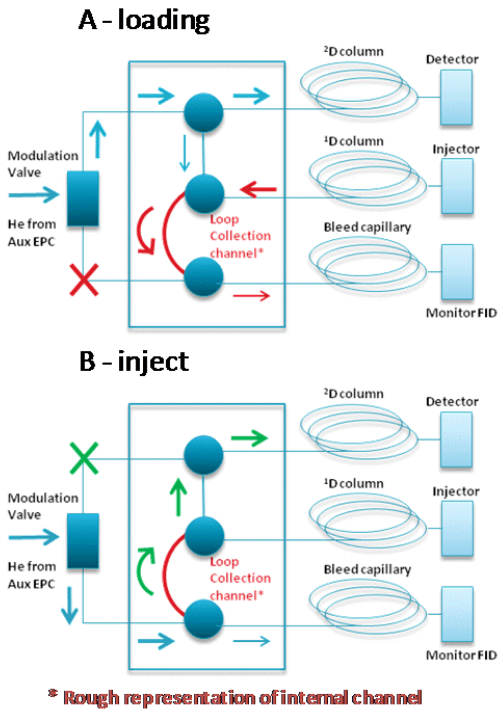

16
17

Figure 2

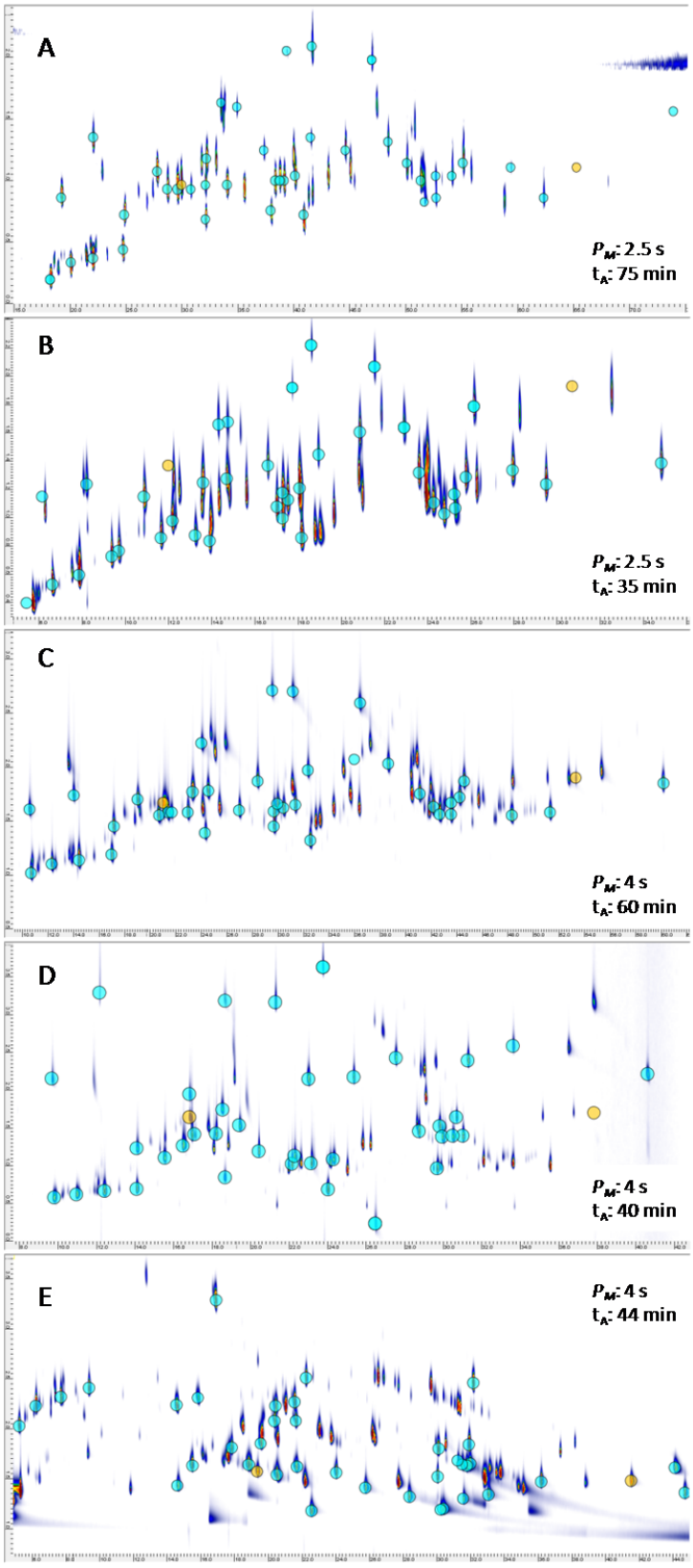
A
P_M: 2.5 s
t_A: 75 min
B
P_M: 2.5 s
t_A: 35 min
C
P_M: 4 s
t_A: 60 min
D
P_M: 4 s
t_A: 40 min
E
P_M: 4 s
t_A: 44 min

Figure 3

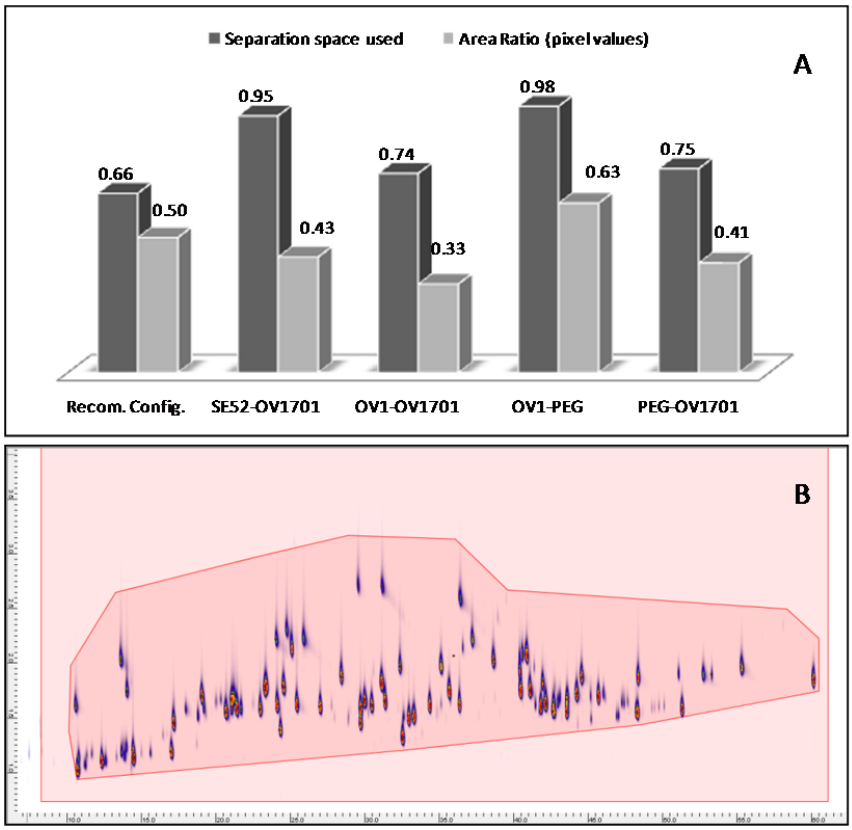

19
20

Figure 4

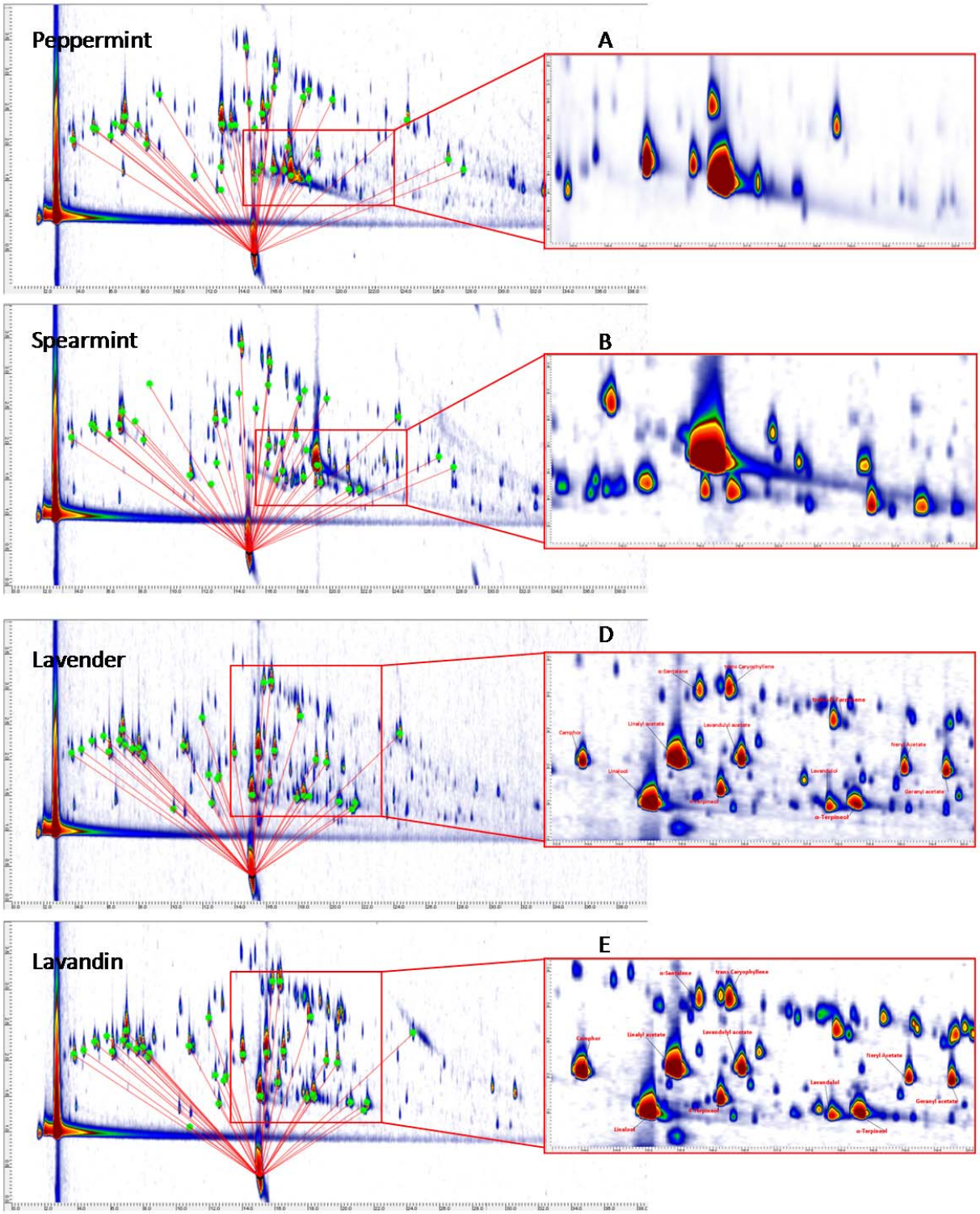

Figure 5

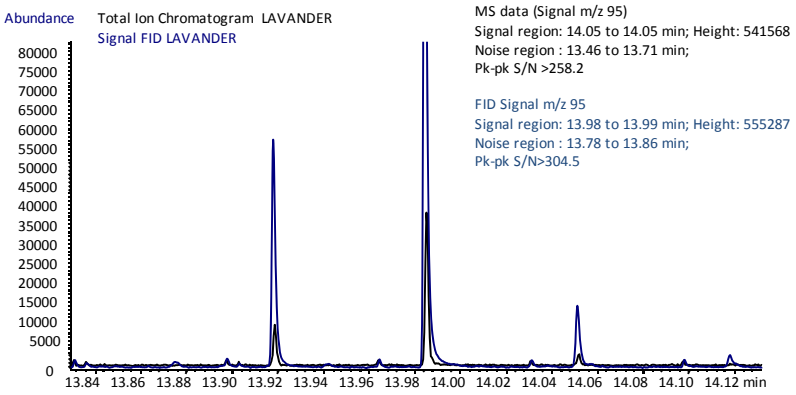

23
24

Figure 6

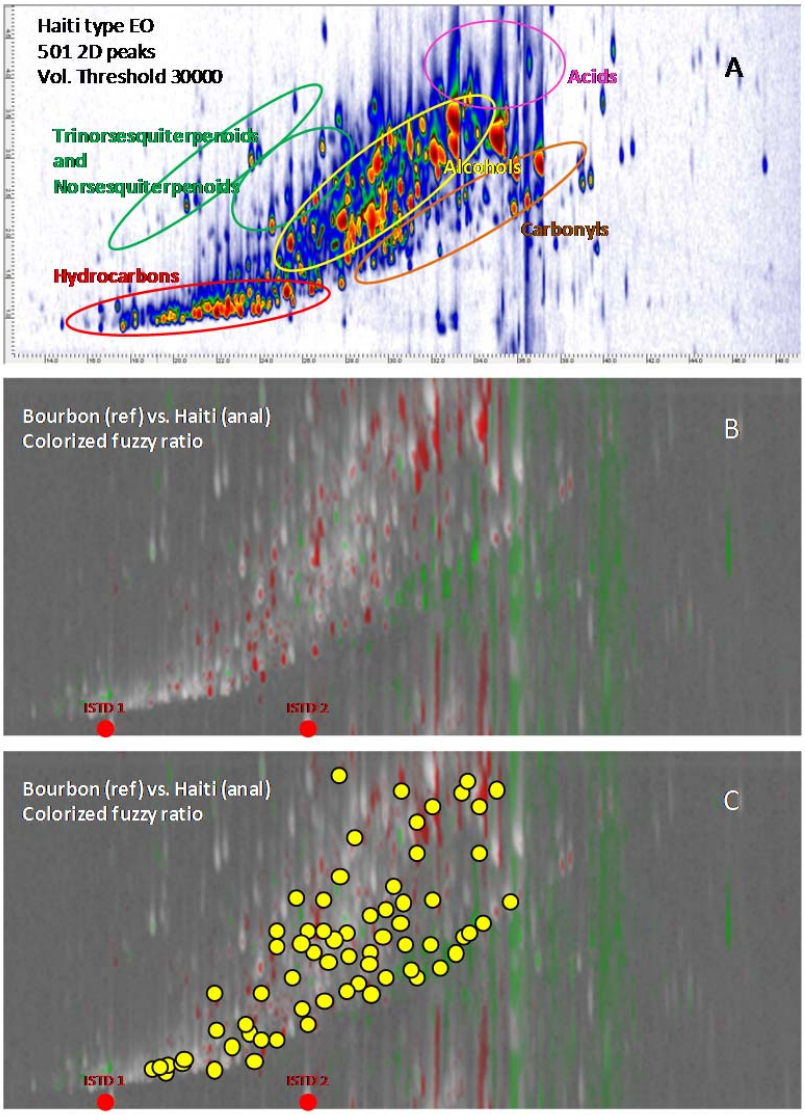

25
26

27

28 **References**

[1] D. Lamparsky in: P. Sandra, C. Bicchi (Eds.), Capillary Gas Chromatography in Essential Oil analysis, Dr. Alfred Huethig Verlag, Heidelberg 1987, pp 155-213

[2] J. C. Giddings, Sample dimensionality: a predictor of order-disorder in component peak distribution in multidimensional separation, J. Chromatogr. A 703 (1995) 3-15

[3] C. Bicchi, M. Maffei, The plant volatilome: Methods of analysis, Methods Mol Biol. 918 (2012) 289-310

[4] C. Cordero, J. Kiefl, S.E. Reichenbach, P. Schieberle, C. Bicchi, Comprehensive two-dimensional gas chromatography and food sensory properties: potential and challenges, Anal. Bioanal. Chem. 407 (2015) 169-191

[5] M. Adahchour, J. Beens, R.J.J. Vreuls, U.A.Th. Brinkman, Recent developments in comprehensive two-dimensional gas chromatography (GC× GC): I. Introduction and instrumental set-up, Trends Anal. Chem. 25 (2006) 438-454.

[6] H.J. Cortes, B. Winniford, J. Luong, M. Pursch, Comprehensive two dimensional gas chromatography review, J. Sep. Sci. 32 (2009) 883-904.

[7] M. Klee, J. Cochran, M. Merrick, L.M. Blumberg, Evaluation of conditions of comprehensive two-dimensional gas chromatography that yield a near-theoretical maximum in peak capacity gain, J. Chromatogr. A, 1383 (2015) 151-159

[8] P.Q. Tranchida, G.Pucaro, P.Dugo, L. Mondello, The modulators for comprehensive two-dimensional gas chromatography:a review, Trends Anal. Chem. 30 (2011) 1347-1461

[9] C. Cordero, S. A.Zebelo, G. Gnavi, A. Griglione, C. Bicchi, M. E. Maffei, P. Rubiolo, HS-SPME-GC×GC-qMS volatile metabolite profiling of *Chrysolina herbacea* frass and *Mentha* spp. leaves. Anal. Bioanal. Chem. 402 (2012) 1941-1952.

[10] P. Rubiolo, B. Sgorbini, E. Liberto, C. Cordero, C. Bicchi, Essential oils and volatiles: Sample preparation and analysis. A review. Flavour Frag. J. 25 (2010) 282-290.

[11] J. V. Seeley, Recent advances in flow-controlled multidimensional gas chromatography, J. Chromatogr. A 1255 (2012) 24-37.

[12] J.V. Seeley, S.K. Seeley, Multidimensional gas chromatography: fundamental advances and new applications, Anal Chem 85 (2013) 557-578.

[13] M. Klee, L.M. Blumberg A critical assessment of the current status and potential future of GC×GC, Proceedings of the ISCC & 11th GC×GC 2014 Riva del Garda, Italy

[14] P.A. Bueno, J.V. Seeley, Flow-switching device for comprehensive two-dimensional gas chromatography, J. Chromatogr A 1027 (2004) 3-10.

[15] J. V. Seeley, N. J. Micyus, J. D. McCurry, S. K. Seeley, Comprehensive Two-Dimensional Gas Chromatography with a Simple Fluidic Modulator,Am. Lab. 38 (2006) 24−26

[16] P.Q. Tranchida, F.A Franchina, P. Dugo, L. Mondello, Use of greatly-reduced gas flows in flow-modulated comprehensive two-dimensional gas chromatography-mass spectrometry, J. Chromatogr. A 1359 (2014) 271-276.

[17] P.Q. Tranchida, F.A Franchina, P. Dugo, L. Mondello. Flow-modulation low-pressure comprehensive two-dimensional gas chromatography, J. Chromatogr A 1372 (2014) 236-244

[18] Q. Gu, F. David, F. Lynen, K. Rumpel, G. Xu, P. De Vos, P. Sandra, Analysis of bacterial fatty acids by flow modulated comprehensive two-dimensional gas chromatography with parallel flame ionization detector/mass spectrometry, J. Chromatogr. A 1217 (2010) 4448–4453

[19] G. Semard, C. Gouin, J. Bourdet, N. Bord, V. Livadaris, Comparative study of differential flow and cryogenic modulators comprehensive two-dimensional gas chromatography systems for the detailed analysis of light cycle oil, J. Chromatogr. A 1218 (2011) 3146–3152

[20] J. Krupcík, R. Gorovenko, I. Špánik, P. Sandra, D.W. Armstrong, Flow-modulated comprehensive two-dimensional gas chromatography with simultaneous flame ionization and quadrupole mass spectrometric detection, J. Chromatogr. A 1280 (2013) 104– 111

[21] P. Manzano, J. C. Diego, J. L. Bernal, M.J. Nozal, J. Bernal, Comprehensive two-dimensional gas chromatography coupled with static headspace sampling to analyze volatile compounds: Application to almonds, J. Sep. Sci. 37 (2014) 675–683

[22] J.F. Griffith, W.L. Winniford, K. Sun, R. Edam, J.C. Luong, A reversed-flow differential flow modulator for comprehensive two-dimensional gas chromatography, J. Chromatogr. A 1226 (2012) 116– 123

[23] C. Duhamel, P. Cardinael, V. Peulon-Agasse, R. Firor, L. Pascaud, G. Semard-Jousset, P. Giusti, V. Livadaris, Comparison of cryogenic and differential flow (forward and reverse fill/flush) modulators and applications to the analysis of heavy petroleum cuts by high-temperature comprehensive gas chromatography, J. Chromatogr. A 1387 (2015) 95–103

[24] Y. de Saint Laumer, E. Cicchetti, P. Merle, J. Egger, A. Chaintreau, Quantification in gas chromatography: prediction of flame ionization detector response factors from combustion enthalpies and molecular structures, Anal. Chem. 82 (2010) 6457-6462

[25] European Pharmacopoeia VIII ed. 2014 - European Directorate for the Quality of Medicines (EDQM)

[26] J. Beens, M. Adahchour, R.J.J. Vreuls, K. van Altena, U.A.Th. Brinkman, Simple, non-moving modulation interface for comprehensive two-dimensional gas chromatography, J. Chromatogr. A 919 (2001) 127-132

[27] L. M. Blumberg, M. S. Klee, Metrics of separation in chromatography, J. Chromatogr. A 933 (2001) 1 -11.

[28] L. M.Blumberg, Comprehensive two-dimensional gas chromatography: metrics, potentials, limits, J. Chromatogr. A 985 (2003) 29 – 38.

[29] C. Cordero, C. Bicchi, M. Galli, S. Galli, P. Rubiolo, Evaluation of different internal-diameter column combinations in comprehensive two-dimensional gas chromatography in flavour and fragrance analysis, J. Sep. Sci. 31 (2008) 3437 -3450

[30] W. Khummueng, J. Harynuk, P.J. Marriott, Modulation ratio in comprehensive two-dimensional gas chromatography, Anal. Chem. 78 (2006) 4578 – 4587.

[31] D. Ryan, P. Morrison, P. Marriott, Orthogonality considerations in comprehensive two-dimensional gas chromatography, J. Chromatogr. A. 1071 (2005) 47 – 53

[32] J.J. Filippi, E. Belhassen, N. Baldovini, H. Brevard, U. Meierhenrich, Qualitative and quantitative analysis of vetiver essential oils by comprehensive two-dimensional gas chromatography and comprehensive two-dimensional gas chromatography/mass spectrometry, J. Chromatogr. A. 1288 (2013) 127-148.

[33] B. Sgorbini, C. Cagliero, L. Boggia, E. Liberto, S.E. Reichenbach, P. Rubiolo, C. Cordero, C. Bicchi, Parallel dual secondary-column-dual detection comprehensive two-dimensional gas chromatography: A flexible and reliable analytical tool for essential oils quantitative profiling. Flavour Fragr. J. 2015 in press DOI: 10.1002/ffj.3255.

[34] D. Bressanello, E. Liberto, M. Collino, S.E. Reichenbach, E. Benetti, F. Chiazza, C. Bicchi, C. Cordero, Urinary metabolic fingerprinting of mice with diet-induced metabolic derangements by parallel dual secondary column-dual detection two-dimensional comprehensive gas chromatography, J. Chromatogr. A. 1361 (2014) 265-276

[35] B. Lawrence ed. Mint The genus *Mentha* - Medicinal and Aromatic Plants — Industrial Profiles- CRC Press 2007 Boca Raton (FL, US)

[36] International Organization for Standardization (2002). ISO 3515, Oil of lavender (*Lavandula angustifolia* Mill). ISO, Geneva

[37] International Organization for Standardization (2006). ISO 856, Oil of peppermint (*Mentha* x *piperita* L.) ISO, Geneva, 12 pp

[38] E. Belhassen, J.J. Filippi, H. Brevard, D. Joulain, N. Baldovini, Volatile constituents of vetiver: a review, Flavour Fragr. J. 30 (2015) 26–82

[39] P. Marriott, R. Shellie, J. Fergeus, R. Ong, P. Morrison, High resolution essential oil analysis by using comprehensive gas chromatographic methodology, Flavour Fragr. J. 15 (2000) 225-239.

[40] International Organization for Standardization (2013). ISO 4716, Essential oil of vetiver [*Chrysopogon zizanioides* (L.) Roberty, syn. *Vetiveria zizanioides* (L.) Nash] ISO, Geneva, 11 pp

[41] S.E. Reichenbach, X. Tian, C. Cordero, Q. Tao, Features for non-targeted cross-sample analysis with comprehensive two-dimensional chromatography, J. Chromatogr. A 1226 (2012) 140-148

[42] S.E. Reichenbach, X. Tian, Q. Tao, E. Ledford, Z. Wu, O. Fiehn, Informatics for cross-sample analysis with comprehensive two-dimensional gas chromatography and high-resolution mass spectrometry (GC×GC-HRMS), Talanta 83 (2011)1279-1288

[43] S.E. Reichenbach, X. Tian, A.A. Boateng, C.A. Mullen, C. Cordero, Q. Tao, Reliable peak selection for multisample analysis with comprehensive two-dimensional chromatography, Anal Chem. 85 (2013) 4974-4981